EUROPEAN JOURNAL OF PURE AND APPLIED MATHEMATICS
2025, Vol. 18, Issue 4, Article Number 6884
ISSN 1307-5543 – ejpam.com
Published by New York Business Global

Fuzzy Fractal-Fractional Derivative-Based Modelling and Analysis of Monkeypox Transmission

Vediyappan Govindan[1], Busayamas Pimpunchat[2,*], Kamran[3,*], Mohammad Javad Ebadi[4], Ioan-Lucian Popa[5,6]

[1] *Department of Mathematics, Hindustan Institute of Technology and Science, Chennai, India*
[2] *Department of Mathematics, School of Science, King Mongkut's Institute of Technology Ladkrabang (KMITL), Bangkok, 10520, Thailand*
[3] *Department of Mathematics, Islamia College Peshawar, Peshawar 25120, Khyber Pakhtunkhwa, Pakistan*
[4] *Department of Mathematics, Chabahar Maritime University, Chabahar, Iran*
[5] *Department of Computing, Mathematics and Electronics, "1 Decembrie 1918" University of Alba Iulia, 510009 Alba Iulia, Romania*
[6] *Faculty of Mathematics and Computer Science, Transilvania University of Brasov, Iuliu Maniu Street 50, 500091 Brasov, Romania*

Abstract. This study investigates the transmission dynamics of monkeypox using a fuzzy fractal fractional-order mathematical model. The model incorporates fuzzy triangular numbers into both system parameters and initial conditions to effectively represent uncertainty in real-world epidemiological data. By employing fractal-fractional derivatives, the model captures memory and hereditary effects, providing a more accurate representation of disease progression. The mathematical analysis, supported by Ulam-Hyers stability and fixed-point theory, confirms the model's reliability. Numerical simulation reveals the effects of changing the fractional order and uncertain inputs on the susceptible, exposed, infected, and recovered populations. The results underscore the enhanced comprehension of monkeypox spread and recovery provided by the combined effects of fractional dynamics and fuzziness and provide important insights for public health policy.

2020 Mathematics Subject Classifications: 26A33, 34A08, 92D30, 03E72

Key Words and Phrases: Mathematical model, fractal fractional operator, fuzzy values, triangular fuzzy number, Lipschitz function, Ulam-Hyers stability

*Corresponding author.
*Corresponding author.
DOI: https://doi.org/10.29020/nybg.ejpam.v18i4.6884

Email addresses: busayamas.pi@kmitl.ac.th (B. Pimpunchat), kamran.maths@icp.edu.pk (Kamran)

1. Introduction

Mpox, previously referred to as monkeypox, is an emerging viral infection with growing worldwide importance. The CDC (2024) reports its prevention, management, and spread [1]. A WHO-sponsored study by Hoxha et al. (2023) reported Mpox infections in children during the outbreak in 2022–2023, citing distinct clinical findings [2]. Lu et al. (2023) offered a review of Mpox pathogenesis and therapy, focusing on vaccine and antiviral improvements [3]. Karagoz et al. (2023) presented in detail the origin, genome, transmission, and diagnostic methods of the virus [4]. The WHO (2024) is still publishing global health advice and prevention measures [5]. Mpox re-emerged in 2022 with a worldwide epidemic that had predominantly beset the MSM population in the presentation of genital ulcers and lymphadenopathy [6]. Transmission is caused by direct contact with an infected lesion, body fluids, respiratory droplets, or contaminated material. Although previously rare, human-to-human transmission is now recognized as a significant mode of spread. Preventive strategies include isolation, symptomatic treatment, and post-exposure vaccination with the modified vaccinia Ankara (MVA) vaccine, which has shown a favourable safety profile even in immunocompromised individuals [7]. Enhanced surveillance, vaccination strategies, and global awareness are essential in mitigating the ongoing outbreak and addressing the challenges posed by this re-emerging disease.

Researchers in infectious diseases have highlighted the significant role of mathematics and mathematical modelling in providing a clear framework for understanding the transmission dynamics of infectious diseases among individuals, communities, and animal populations. They have developed simplified models that incorporate essential clinical and biological parameters to describe disease development and spread [8–11]. In this context, numerous mathematical studies have examined the dynamics of various epidemic phenomena, such as alcoholism, smoking, COVID-19, and obesity [12–19].

To study the dynamics of monkeypox specifically, several compartmental models commonly used in epidemiology have been proposed [20–22]. Although monkeypox received limited attention in the past, leading to gaps in understanding its transmission mechanisms, more recent studies have started to address this issue through mathematical modelling techniques. A deterministic mathematical model was developed in [23] to examine the monkeypox outbreak, revealing that isolating infected individuals significantly reduces disease incidence. A system of nonlinear differential equations was proposed in [24] to analyse multiple transmission pathways of monkeypox.

Several foundational studies have contributed to understanding monkeypox transmission dynamics. For instance, the transmission dynamics of pox-like diseases using monkeypox as a case study were first analysed in [25]. The potential for eradication of monkeypox from both human and non-human primate populations through structured treatment interventions was demonstrated in [26]. A detailed stability analysis involving both human hosts and rodents was carried out in [27]. Additional contributions using compartmental modelling to enhance the understanding of monkeypox dynamics can be found in [28, 29]. In [30] considered both human-to-human and rodent-to-human transmission, offering an in-depth analysis without relying on specific outbreak data.

Recent studies have introduced innovative approaches to modelling monkeypox dynamics. A study [31] analyses backward bifurcation using real observed data, highlighting how key parameters influence disease persistence. Another work [32] examines the transmission dynamics of the monkeypox virus using compartmental models to identify critical factors in its spread. Additionally, optimal control strategies have been applied in [33] to evaluate the effectiveness of interventions such as vaccination and isolation in reducing infection rates. Fractional-order differential equations have gained prominence in epidemiology due to their ability to capture memory and hereditary effects, which classical models often overlook [34–38]. This approach has been used to model both infectious and non-infectious diseases, including COVID-19 [39–41]. In the context of monkeypox, a stochastic model addressing cross-infection was proposed in [42], and zoonotic transmission using fractal-fractional operators was explored in [43]. Fractional-order operators like the Mittag–Leffler kernel and Caputo–Fabrizio derivative have improved model accuracy in various epidemiological studies [44–46]. Specifically, monkeypox spread in Nigeria was modeled using real data in [47], highlighting the role of public health measures, while [48] emphasized the importance of isolating infected individuals to reduce transmission.

Fuzzy logic has also been applied in epidemic modelling to manage uncertainty in parameters. The impact of fuzzy transmission and treatment rates was studied in [49], while [50] conducted sensitivity analysis under fuzzy imprecision. Combining fuzzy logic with fractional calculus enhances model realism, as demonstrated in fuzzy fractional COVID-19 models [51, 52] and malaria modelling [53]. Theoretical advancements in fuzzy fractional operators have been presented in [54], along with efficient numerical methods for solving such systems [55].

This research introduces a new fuzzy fractal fractional-order model to study the spread of monkeypox. It is the first approach that combines fuzzy logic with fractal-fractional derivatives to analyse disease transmission. Unlike existing models, this framework uniquely integrates fuzzy triangular numbers into model parameters and initial conditions, effectively capturing the imprecision and uncertainty present in real-world epidemiological data. The use of fractal-fractional operators allows the model to capture memory effects and genetic factors, making the analysis more realistic and detailed. The study also makes additional contributions by developing the theoretical validity of the intended model using fixed-point theory and Ulam-Hyers stability to guarantee the consistency of the system. Numerical computations illustrate the impact of varying fractional orders and fuzzy values on main population compartments (susceptible, exposed, infected, recovered), thereby highlighting the model's ability to reflect complex disease behaviour more accurately than classical or purely fractional models. This integrated modelling framework provides valuable insights for designing effective public health strategies against monkeypox, making it a significant advancement in epidemic modelling literature.

2. Preliminaries

This section presents the essential definitions and foundational concepts related to fractal-fractional differential equations and fuzzy systems, which serve as the theoretical

basis for this study. The treatment of fractional differential equations under uncertainty is examined in the work of [56], while the formulation of fuzzy differential equations and fractional differential equations with fuzzy initial conditions is detailed in [57, 58]. Collectively, these studies provide the theoretical framework underpinning the present research.

Definition 1. *The fuzzy set A consists of arranged collections $A = \{(x, \mu_A(x)) : x \in X\}$, and the value or grade $\mu_A(x)$ of a membership function is an element from $X \to [0, 1]$.*

Definition 2. *The Triangular Fuzzy Number represented by three numbers $\breve{a}$, $\breve{b}$, $\breve{c}$ has its membership function defined as*

$$\mu_A(x) = \begin{cases} \frac{x-\breve{a}}{\breve{b}-\breve{a}} & \text{if } \breve{a} \le x \le \breve{b} \\ \frac{\breve{c}-x}{\breve{c}-\breve{b}} & \text{if } \breve{b} \le x \le \breve{c} \\ 0 & \text{otherwise,} \end{cases}$$

where $\breve{a} \le \breve{b} \le \breve{c}$. Therefore $A = (\breve{a}, \breve{b}, \breve{c})$ can be defined as illustrated in [59]. An α-cut of fuzzy number $\tilde{A}$ can be expressed by

$$[\tilde{A}_l(\alpha), \tilde{A}_r(\alpha)] = [(1-\alpha)\breve{a} + \alpha\breve{b}, (1-\alpha)\breve{c} + \alpha\breve{b}], \quad \forall \alpha \in [0, 1].$$

Definition 3. *A fuzzy set $\tilde{A}$ has an associated α-cut at level $\alpha \in [0, 1]$, which is the crisp subset of X containing all elements whose membership degree exceeds or is equivalent to α, i.e.,*

$$\tilde{A}_\alpha = \{x \in X \mid \tilde{A}(x) \ge \alpha\}, \quad \alpha \in [0, 1].$$

Definition 4. *(Graded Mean Integral Value Theorem [60]). Let $m \in [0, 1]$ be the optimism degree for a fuzzy number. Now, for a fuzzy number $\tilde{A}$, the graded mean integral value (GMIV) is defined in turn.*

$$G_f(\tilde{A}) = \frac{\int_0^1 t_f \left\{(1-m)I_L^{-1}(t_f) + mI_R^{-1}(t_f)\right\} dt}{\int_0^1 t_f \, dt} = 2\int_0^1 t_f \left\{(1-m)I_L^{-1}(t_f) + mI_R^{-1}(t_f)\right\} dt,$$

where I_L and I_R are the left and right integral values of a fuzzy number $\tilde{A}$.

For triangular membership function,

$$I_L(t_f) = \frac{t_f - \breve{a}}{\breve{b} - \breve{a}}, \quad \text{and} \quad I_R(t_f) = \frac{\breve{c} - t_f}{\breve{c} - \breve{b}},$$

$$I_L^{-1}(t_f) = \breve{a} + (\breve{b} - \breve{a})t_f, \quad I_R^{-1}(t_f) = \breve{c} - (\breve{c} - \breve{b})t_f.$$

Therefore, the GMIV is given as

$$\tilde{A} = 2\int_0^1 t_f \left\{(1-m)I_L^{-1}(t_f) + mI_R^{-1}(t_f)\right\} dt_f = \frac{1}{3}[(1-m)\breve{a} + 2\breve{b} + m\breve{c}].$$

Definition 5. *Consider a function $f : X \to Y$ be such that X and Y are crisp sets. Let $\tilde{A}$ and $\tilde{B}$ be fuzzy sets on X and Y respectively. If the membership values satisfy the condition $\mu_{\tilde{A}}(x) \leq \mu_{\tilde{B}}(x)$, then the function is termed a fuzzy function with constraints defined over the fuzzy domain $\tilde{A}$ and fuzzy range $\tilde{B}$.*

Definition 6. *Given a fuzzy number $\tilde{V}$, its β-level set is defined as*

$$[\tilde{V}]^{\beta} = \{x \in \mathbb{R} \mid \tilde{V}(x) \geq \beta\},$$

where $\beta \in (0, 1]$ and $x \in \mathbb{R}$.

Definition 7. *A fuzzy number can be described using a parametric form as a pair $[\underline{V}(\omega), \overline{V}(\omega)]$ where $0 \leq \omega \leq 1$, satisfying the following conditions:*

- *$\underline{V}(\omega)$ is a bounded and non-decreasing function, which is right-continuous at 0, and left-continuous for $(0, 1)$.*
- *$\overline{V}(\omega)$ is a non-increasing and bounded function on $[0, 1]$, right-continuous at 0.*
- *It always holds that $\underline{V}(\omega) \leq \overline{V}(\omega)$.*
- *When $\underline{V}(\omega) = \overline{V}(\omega) = 0$, the fuzzy number becomes a crisp value.*

Definition 8. *Consider a function $\alpha : E \times E \to \mathbb{R}$, let two fuzzy numbers be $p = (\underline{p}(\omega), \overline{p}(\omega))$ and $q = (\underline{q}(\omega), \overline{q}(\omega))$. The Hausdorff-type metric $\alpha(p, q)$ is defined by:*

$$\alpha(p, q) = \sup_{\omega \in [0,1]} \max \left\{ |\underline{p}(\omega) - \underline{q}(\omega)|, |\overline{p}(\omega) - \overline{q}(\omega)| \right\}.$$

This function satisfies the properties below:

- *$\alpha(p + q, q + p) = \alpha(p, q)$ for all $p, q \in E$.*
- *$\alpha(p\varrho, q\varrho) = |\varrho|\alpha(p, q)$ for all $p, q \in E$, with $\varrho \in \mathbb{R}$.*
- *$\alpha(p + r, q + s) \leq \alpha(p, q) + \alpha(r, s)$ for all $p, q, r, s \in E$.*

The space (E, α) form a complete metric space.

Definition 9. *If two fuzzy numbers $i_1, i_2 \in E$ satisfy the relation $i_1 = i_2 + i_3$ for some fuzzy number $i_3 \in E$, then i_3 is called the H-difference of i_1 and i_2, and is denoted by $i_1 \ominus i_2$.*

Definition 10. *Consider a fuzzy-valued function $\Theta : \mathbb{R} \to E$. The function Θ is said to be continuous at a point $\Lambda_0 \in [\zeta_1, \zeta_2]$, if for any $\varepsilon > 0$, there exists $\delta > 0$ such that:*

$$\alpha(\Theta(\Lambda), \Theta(\Lambda_0)) < \varepsilon \quad \textit{whenever} \quad |\Lambda - \Lambda_0| < \delta.$$

Definition 11. *Let $\omega(x)$ be a fuzzy function belongs to $C^{\mathfrak{F}}[0,b] \cap L^{\mathfrak{F}}[0,b]$, and represented as $\omega = [\underline{\omega}_p(x), \overline{\omega_p}(x)]$ for $0 \leq p \leq 1$. The Caputo type fuzzy fractional derivative is:*

$$[D^{\beta}\omega(x_0)]_p = [D^{\beta}\underline{\omega}_p(x_0), D^{\beta}\overline{\omega_p}(x_0)], \quad 0 \leq \beta \leq 1,$$

where

$$D^{\beta}\underline{\omega}_p(x_0) = \frac{1}{\Gamma(n-\beta)}\left[\int_0^x (x-\zeta)^{n-\beta-1}\frac{d^n}{d\zeta^n}\underline{\omega}_p(\zeta)\,d\zeta\right]_{x=x_0},$$

$$D^{\beta}\overline{\omega_p}(x_0) = \frac{1}{\Gamma(n-\beta)}\left[\int_0^x (x-\zeta)^{n-\beta-1}\frac{d^n}{d\zeta^n}\overline{\omega_p}(\zeta)\,d\zeta\right]_{x=x_0}.$$

With $n = \lceil \beta \rceil$ provided the integral exists.

Definition 12. *Suppose a fuzzy function $\tilde{U}$ is defined as $\tilde{U} = [\underline{U}_p(x), \overline{U_p}(x)]$ for $0 \leq p \leq 1$. The Riemann-Liouville type Fuzzy fractal fractional derivative involving the generalized Mittag-Leffler Kernel function is given by*

$$({}_0^{FFM})D_{\tau}^{(\eta,\vartheta)}(\tilde{U}(\tau)) = \frac{\mathcal{AB}(\vartheta)}{1-\vartheta}\frac{d}{dt^{\eta}}\int_0^{\tau} E_{\vartheta}\left[-\frac{\vartheta}{1-\vartheta}(\tau-\psi)^{\vartheta}\tilde{U}(\psi)\,d\psi\right]. \tag{1}$$

Where $0 < \vartheta, \eta \leq 1$ and $\mathcal{AB}(\vartheta) = 1 - \vartheta + \frac{\vartheta}{\lceil \vartheta \rceil}$.

The associated integral operator for this derivative is defined as:

$$({}_0^{FFM})I_{\tau}^{(\eta,\vartheta)}(\tilde{U}(\tau)) = \frac{\eta(1-\vartheta)\tau^{\eta-1}\tilde{U}(\tau)}{\mathcal{AB}(\vartheta)} + \frac{\eta\vartheta}{\mathcal{AB}(\vartheta)\lceil\vartheta\rceil} \times \int_0^{\tau} \psi^{\eta-1}(\tau-\psi)^{\vartheta-1}\tilde{U}(\psi)\,d\psi. \tag{2}$$

3. Model Formulation

This section formulates a fuzzy fractal-fractional mathematical framework to study monkeypox disease dynamics considering interactions between human-animal populations. The operator of the fractional derivative Atangana-Baleanu-Caputo (ABC), involving memory effects as well as local behaviours in existence within biological environments, is adopted in the proposed model. To further enhance the model's realism, fuzzy set theory is employed to account for uncertainty and imprecision in parameter estimation, such as contact rates, recovery rates, and transition probabilities. Moreover, the model integrates fractal dimension through a fractal-fractional framework, allowing a more generalized and flexible representation of the complex dynamics of disease spread across heterogeneous populations. By merging these higher-level mathematical tools, the model offers a strong and inclusive framework for analysing the dynamics and control of monkeypox in an uncertain and complex biological memory environment.

3.1. Evolution of Human Population

There are various compartments in the human population:

- $S_H(\tau)$: Susceptible humans

- $I_H(\tau)$: Infected humans
- $T_H(\tau)$: Treated (or isolated) humans
- $R_H(\tau)$: Recovered humans
- $P_H(\tau)$: Protected humans

Let $N_H = S_H(\tau) + I_H(\tau) + T_H(\tau) + R_H(\tau) + P_H(\tau)$ denote the total human population. The Atangana-Baleanu logic of a Fractal-Fractional derivative regulates the propagation dynamics, and the power-law kernel is defined as $({}_0^{FFM})D_\tau^{(\eta,\vartheta)}$. The model of the human population is provided by the given system of fractional differential equations:

$$\begin{aligned}
({}_0^{FFM})D_\tau^{(\eta,\vartheta)} S_H(\tau) &= \Pi_H - \lambda_H S_H - (\mu_H + \xi_H) S_H \\
({}_0^{FFM})D_\tau^{(\eta,\vartheta)} I_H(\tau) &= \lambda_H S_H - (\Upsilon_H + \mathcal{E}_1 + \delta_1 + \omega_H + \mu_H) I_H \\
({}_0^{FFM})D_\tau^{(\eta,\vartheta)} T_H(\tau) &= \Upsilon_H I_H - (\mathcal{E}_2 + \delta_2 + \mu_H) T_H \\
({}_0^{FFM})D_\tau^{(\eta,\vartheta)} R_H(\tau) &= \mathcal{E}_1 I_H + \mathcal{E}_2 T_H - (\mu_H + \theta_H) R_H \\
({}_0^{FFM})D_\tau^{(\eta,\vartheta)} P_H(\tau) &= \xi_H S_H + \omega_H I_H + \theta_H R_H - \mu_H P_H.
\end{aligned}$$

Where

- Π_H: Recruitment rate into the human population
- λ_H: Force of infection combining contact with infected animals and humans
- μ_H: Natural human death rate
- ξ_H: Susceptible individuals' rate entering the protected class to avoid infection
- Υ_H: Infection cases' rate entering treatment or isolation
- $\mathcal{E}_1, \mathcal{E}_2$: Recovery rates from infection and treatment, respectively
- δ_1, δ_2: Disease-induced death rates from infected and treated individuals
- ω_H: Rate at which infection cases are transferred into protection in order to prevent further spread
- θ_H: Recovery rate at which cured persons shift to the protected class

This structure captures the dynamic transitions in the human population, integrating memory and non-local effects via the fractal-fractional operator.

3.2. Animal Population Dynamics

The animal population is divided into:

- $S_A(\tau)$: Susceptible animals
- $I_A(\tau)$: Infected animals
- $R_A(\tau)$: Recovered animals.

Let $N_A = S_A + I_A + R_A$ be the total animal population.

The animal model follows a similar nonlinear system of differential equations based on classical or fractional derivatives (depending on your specification):

$$\begin{aligned}
({}_0^{FFM})D_\tau^{(\eta,\vartheta)} S_A(\tau) &= \Pi_A - \lambda_A S_A - \mu_A S_A \\
({}_0^{FFM})D_\tau^{(\eta,\vartheta)} I_A(\tau) &= \lambda_A S_A - (\Upsilon_A + \mu_A + d_A) I_A \\
({}_0^{FFM})D_\tau^{(\eta,\vartheta)} R_A(\tau) &= \Upsilon_A I_A - \mu_A R_A.
\end{aligned}$$

Where

- Π_A: Recruitment rate into the animal population
- λ_A: Contact rate between infected and susceptible animals that combines into force of infection
- μ_A: Animal natural death rate
- d_A: Mortality rate due to disease in animals
- Υ_A: Rate of recovery of infected animals.

This model framework facilitates a comprehensive exploration of monkeypox transmission dynamics and control strategies within a fractional-order setting, effectively capturing the influence of memory and hereditary behaviour in population of humans and animals. The corresponding equations are formulated using a fractal-fractional framework characterized by the order η $(0 < \eta < 1)$ and fractal dimension ϑ.

The model also uses fuzzy initial conditions to reflect the uncertainty and imprecision associated with the starting values of each compartment, ensuring a more realistic and flexible simulation framework.

$$
\begin{aligned}
({}_0^{FFM})D_\tau^{(\eta,\vartheta)}S_H(\tau) &= (\tilde{\Pi_H}) - (\tilde{\lambda_H})S_H - ((\tilde{\mu_H}) + (\tilde{\xi_H}))S_H \\
({}_0^{FFM})D_\tau^{(\eta,\vartheta)}I_H(\tau) &= (\tilde{\lambda_H})S_H - ((\tilde{\Upsilon_H}) + (\tilde{\mathcal{E}_1}) + (\tilde{\delta_1}) + (\tilde{\omega_H}) + (\tilde{\mu_H}))I_H \\
({}_0^{FFM})D_\tau^{(\eta,\vartheta)}T_H(\tau) &= (\tilde{\Upsilon_H})I_H - ((\tilde{\mathcal{E}_2}) + (\tilde{\delta_2}) + (\tilde{\mu_H}))T_H \\
({}_0^{FFM})D_\tau^{(\eta,\vartheta)}R_H(\tau) &= (\tilde{\mathcal{E}_1})I_H + (\tilde{\mathcal{E}_2})T_H - ((\tilde{\mu_H}) + (\tilde{\theta_H}))R_H \\
({}_0^{FFM})D_\tau^{(\eta,\vartheta)}P_H(\tau) &= (\tilde{\xi_H})S_H + (\tilde{\omega_H})I_H + (\tilde{\theta_H})R_H - (\tilde{\mu_H})P_H \\
({}_0^{FFM})D_\tau^{(\eta,\vartheta)}S_A(\tau) &= (\tilde{\Pi_A}) - (\tilde{\lambda_A})S_A - (\tilde{\mu_A})S_A \\
({}_0^{FFM})D_\tau^{(\eta,\vartheta)}I_A(\tau) &= (\tilde{\lambda_A})S_A - ((\tilde{\Upsilon_A}) + (\tilde{\mu_A}) + (\tilde{d_A}))I_A \\
({}_0^{FFM})D_\tau^{(\eta,\vartheta)}R_A(\tau) &= (\tilde{\Upsilon_A})I_A - (\tilde{\mu_A})R_A.
\end{aligned}
\tag{3}
$$

The transmission terms are given by $(\tilde{\lambda_H}) = \frac{((\tilde{\beta_{H_1}})I_A + (\tilde{\beta_{H_2}})I_H)}{N_H}$ for humans and $(\tilde{\lambda_A}) = \frac{(\tilde{\beta_A})I_A}{N_A}$ for animals, representing the respective force of infection. All related parameters such as $\tilde{\Pi_H}$, $\tilde{\lambda_H}$, $\tilde{\mu_H}$, $\tilde{\xi_H}$, $\tilde{\Upsilon_H}$, $\tilde{\mathcal{E}_1}$, $\tilde{\delta_1}$, $\tilde{\mathcal{E}_2}$, $\tilde{\delta_2}$, $\tilde{\omega_H}$, $\tilde{\theta_H}$, $\tilde{\Pi_A}$, $\tilde{\lambda_A}$, $\tilde{\Upsilon_A}$, $\tilde{\mu_A}$ and $\tilde{d_A}$ are modeled as triangular fuzzy numbers (TFNs) with narrow supports ranges to represent the uncertainty present in real-world scenarios. These parameters define the dynamic behavior of the state variables $S_H \geq 0$, $I_H \geq 0$, $T_H \geq 0$, $R_H \geq 0$, $P_H \geq 0$ for humans and $S_A \geq 0$, $I_A \geq 0$, $R_A \geq 0$ for animals within the fuzzy fractal-fractional monkeypox model.

4. Qualitative analysis

Theorem 1. *The solution paths of the proposed model* (3) *are positive at any time instant in* $\mathbb{R}_+^8$.

Proof. It follows from the model (3) that

$$
\begin{aligned}
({}_0^{FFM})D_\tau^{(\eta,\vartheta)}S_H(\tau)\Big|_{S_H=0} &= (\tilde{\Pi_H}) \geq 0, \\
({}_0^{FFM})D_\tau^{(\eta,\vartheta)}I_H(\tau)\Big|_{I_H=0} &= (\tilde{\lambda_H})S_H \geq 0, \\
({}_0^{FFM})D_\tau^{(\eta,\vartheta)}T_H(t)\Big|_{T_H=0} &= (\tilde{\Upsilon_H})I_H \geq 0, \\
({}_0^{FFM})D_\tau^{(\eta,\vartheta)}R_H(t)\Big|_{R_H=0} &= (\tilde{\mathcal{E}_1})I_H + (\tilde{\mathcal{E}_2})T_H \geq 0, \\
({}_0^{FFM})D_\tau^{(\eta,\vartheta)}P_H(t)\Big|_{P_H=0} &= (\tilde{\xi_H})S_H + (\tilde{\omega_H})I_H + (\tilde{\theta_H})R_H \geq 0, \\
({}_0^{FFM})D_\tau^{(\eta,\vartheta)}S_A(\tau)\Big|_{S_A=0} &= (\tilde{\Pi_A}) \geq 0, \\
({}_0^{FFM})D_\tau^{(\eta,\vartheta)}I_A(\tau)\Big|_{I_A=0} &= (\tilde{\lambda_A})S_A \geq 0, \\
({}_0^{FFM})D_\tau^{(\eta,\vartheta)}R_A(\tau)\Big|_{R_A=0} &= (\tilde{\Upsilon_A})I_A \geq 0.
\end{aligned}
$$

All rates are above-described are nonnegative, as are the solution paths in the non-negative of $\mathbb{R}^8_+$.

5. Existence and Uniqueness of Proposed scheme

This part outlines the existence and uniqueness of the solution to the following fuzzy fractional model. The analysis focuses on a system of fuzzy fractional-order differential equations formulated using the Atangana–Baleanu Caputo operator. To reformulate the system in a more analysable form, the Atangana–Baleanu fractal–fractional operator is applied to transform the set of equations (3). With fixed-point theorems, it is shown that the model admits at least one solution uniquely. In below, the suggested model is discussed, considering fractional differentiation and integration techniques.

$$
\begin{aligned}
({}^{AB}_{0})D^{(\eta,\vartheta)}_{\tau}S_H(\tau) &= \vartheta t^{\vartheta-1}g_1(\tau, S_H, I_H, T_H, R_H, P_H, S_A, I_A, R_A)\\
({}^{AB}_{0})D^{(\eta,\vartheta)}_{\tau}I_H(\tau) &= \vartheta t^{\vartheta-1}g_2(\tau, S_H, I_H, T_H, R_H, P_H, S_A, I_A, R_A)\\
({}^{AB}_{0})D^{(\eta,\vartheta)}_{\tau}T_H(\tau) &= \vartheta t^{\vartheta-1}g_3(\tau, S_H, I_H, T_H, R_H, P_H, S_A, I_A, R_A)\\
({}^{AB}_{0})D^{(\eta,\vartheta)}_{\tau}R_H(\tau) &= \vartheta t^{\vartheta-1}g_4(\tau, S_H, I_H, T_H, R_H, P_H, S_A, I_A, R_A)\\
({}^{AB}_{0})D^{(\eta,\vartheta)}_{\tau}P_H(\tau) &= \vartheta t^{\vartheta-1}g_5(\tau, S_H, I_H, T_H, R_H, P_H, S_A, I_A, R_A)\\
({}^{AB}_{0})D^{(\eta,\vartheta)}_{\tau}S_A(\tau) &= \vartheta t^{\vartheta-1}g_6(\tau, S_H, I_H, T_H, R_H, P_H, S_A, I_A, R_A)\\
({}^{AB}_{0})D^{(\eta,\vartheta)}_{\tau}I_A(\tau) &= \vartheta t^{\vartheta-1}g_7(\tau, S_H, I_H, T_H, R_H, P_H, S_A, I_A, R_A)\\
({}^{AB}_{0})D^{(\eta,\vartheta)}_{\tau}R_A(\tau) &= \vartheta t^{\vartheta-1}g_8(\tau, S_H, I_H, T_H, R_H, P_H, S_A, I_A, R_A).
\end{aligned}
$$

Where the fuzzy functions are $g_1, g_2, g_3, g_4, g_5, g_6, g_7, g_8$ then, for $\gamma \in [0,1]$, model (3) gets the form

$$
\begin{cases}
({}^{FFM}_{0})D^{(\eta,\vartheta)}_{\tau}S_H(\tau) = g_1(\tau, S_H, I_H, T_H, R_H, P_H, S_A, I_A, R_A)\\
({}^{FFM}_{0})D^{(\eta,\vartheta)}_{\tau}I_H(\tau) = g_2(\tau, S_H, I_H, T_H, R_H, P_H, S_A, I_A, R_A)\\
({}^{FFM}_{0})D^{(\eta,\vartheta)}_{\tau}T_H(\tau) = g_3(\tau, S_H, I_H, T_H, R_H, P_H, S_A, I_A, R_A)\\
({}^{FFM}_{0})D^{(\eta,\vartheta)}_{\tau}R_H(\tau) = g_4(\tau, S_H, I_H, T_H, R_H, P_H, S_A, I_A, R_A)\\
({}^{FFM}_{0})D^{(\eta,\vartheta)}_{\tau}P_H(\tau) = g_5(\tau, S_H, I_H, T_H, R_H, P_H, S_A, I_A, R_A)\\
({}^{FFM}_{0})D^{(\eta,\vartheta)}_{\tau}S_A(\tau) = g_6(\tau, S_H, I_H, T_H, R_H, P_H, S_A, I_A, R_A)\\
({}^{FFM}_{0})D^{(\eta,\vartheta)}_{\tau}I_A(\tau) = g_7(\tau, S_H, I_H, T_H, R_H, P_H, S_A, I_A, R_A)\\
({}^{FFM}_{0})D^{(\eta,\vartheta)}_{\tau}R_A(\tau) = g_8(\tau, S_H, I_H, T_H, R_H, P_H, S_A, I_A, R_A).
\end{cases}
\tag{4}
$$

The analysis begins by considering uncertain initial conditions.

$$
\begin{aligned}
\tilde{S_H}(0,\gamma) &= [\underline{S_H}(0,\gamma), \overline{S_H}(0,\gamma)]\\
\tilde{I_H}(0,\gamma) &= [\underline{I_H}(0,\gamma), \overline{I_H}(0,\gamma)]\\
\tilde{T_H}(0,\gamma) &= [\underline{T_H}(0,\gamma), \overline{T_H}(0,\gamma)]
\end{aligned}
$$

$$\tilde{R_H}(0,\gamma) = [\underline{R_H}(0,\gamma), \overline{R_H}(0,\gamma)]$$
$$\tilde{P_H}(0,\gamma) = [\underline{P_H}(0,\gamma), \overline{P_H}(0,\gamma)]$$
$$\tilde{S_A}(0,\gamma) = [\underline{S_A}(0,\gamma), \overline{S_A}(0,\gamma)]$$
$$\tilde{I_A}(0,\gamma) = [\underline{I_A}(0,\gamma), \overline{I_A}(0,\gamma)]$$
$$\tilde{R_A}(0,\gamma) = [\underline{R_A}(0,\gamma), \overline{R_A}(0,\gamma)].$$

The system can be further written as

$$({}_0^{ABR})D_\tau^{(\eta,\vartheta)}\tilde{\Phi}(\tau) = \vartheta\tau^{\vartheta-1}\tilde{\Omega}(\tau,\tilde{\Phi}(\tau)) \quad \text{with} \quad \tilde{\Phi}(0) = \tilde{\Phi}_0.$$

Replacing $({}_0^{ABR})D_\tau^{(\eta,\vartheta)}$ with $({}_0^{ABC})D_\tau^{(\eta,\vartheta)}$, applying the fuzzy fractional integral operator I^ϑ together with the provided initial conditions, the system is reformulated.

$$\tilde{\Phi}(\tau) = \tilde{\Phi}(0,\gamma) + \frac{\vartheta\tau^{\vartheta-1}(1-\eta)}{\mathcal{AB}(\eta)}\Omega(\tau,\tilde{\Phi}(\tau)) + \frac{\eta\vartheta}{\lceil\eta\rceil\mathcal{AB}(\eta)} \times \int_0^\tau m^{\vartheta-1}(\tau-m)^{\eta-1}\Omega(\tau,\tilde{\Phi}(\tau))\,dm. \tag{5}$$

Where

$$\tilde{\Phi}(t) = \begin{cases} S_H(\tau) \\ I_H(t) \\ T_H(t) \\ R_H(t) \\ P_H(t) \\ S_A(t) \\ I_A(t) \\ R_A(\tau), \end{cases} \qquad \tilde{\Phi}(0,\gamma) = \begin{cases} \tilde{S_H}(0,\gamma) \\ \tilde{I_H}(0,\gamma) \\ \tilde{T_H}(0,\gamma) \\ \tilde{R_H}(0,\gamma) \\ \tilde{P_H}(0,\gamma) \\ \tilde{S_A}(0,\gamma) \\ \tilde{I_A}(0,\gamma) \\ \tilde{R_A}(0,\gamma), \end{cases} \qquad \Omega(t,\tilde{\Phi}(t)) = \begin{cases} \psi_1(t,S_H(t)) \\ \psi_2(t,I_H(t)) \\ \psi_3(t,T_H(t)) \\ \psi_4(t,R_H(t)) \\ \psi_5(t,P_H(t)) \\ \psi_6(t,S_A(t)) \\ \psi_7(t,I_A(t)) \\ \psi_7(t,R_A(t)). \end{cases}$$

A Banach Space $\mathcal{I} = C \times C \times C \times C \times C \times C \times C$ is constructed, where $C[0,K]$ denotes the space of continuous functions over the interval $[0,K]$, equipped with the norm:

$$\|\tilde{\Phi}\| = \max_{\tau\in[0,K]} |S_H(\tau), I_H(\tau), T_H(\tau), R_H(\tau), P_H(\tau), S_A(\tau), I_A(\tau), R_A(\tau)|.$$

To examine the existence of a solution, the operator $\psi : \mathcal{I} \to \mathcal{I}$ is defined as follows:

$$\psi(\tilde{\Phi})(\tau) = \tilde{\Phi}(0,\gamma) + \frac{\vartheta\tau^{\vartheta-1}(1-\eta)}{\mathcal{AB}(\eta)}\Omega(\tau,\tilde{\Phi}(\tau)) + \frac{\eta\vartheta}{\lceil\eta\rceil\mathcal{AB}(\eta)} \times \int_0^\tau m^{\vartheta-1}(\tau-m)^{\eta-1}\Omega(\tau,\tilde{\Phi}(\tau))\,dm.$$

Assume the nonlinear function $\Omega(\tau,\tilde{\Phi}(\tau))$ satisfies the Lipschitz conditions and a bounded growth condition. That is, for every $\tilde{\Phi} \in \mathcal{I}$, there exists a constant $C_\Phi > 0$ and G_Φ such that:

$$|\Omega(\tau,\tilde{\Phi}(\tau))| \le C_\Phi|\tilde{\Phi}(\tau)| + G_\Phi.$$

And for all $\tilde{\Phi}_1, \tilde{\Phi}_2 \in \mathcal{I}$, there exists a constant $H_\Phi > 0$ such that:

$$|\Omega(\tau, \tilde{\Phi}_1(\tau)) - \Omega(\tau, \tilde{\Phi}_2(\tau))| \leq H_\Phi |\tilde{\Phi}_1(\tau) - \tilde{\Phi}_2(\tau)|. \tag{6}$$

These conditions are used to establish the uniqueness and stability of the solution for the proposed fuzzy fractal-fractional model under the Atangana–Baleanu framework.

Theorem 2. *On the premise that the conditions* (4) *hold. A continuous mapping* $\Omega : [0, K] \times \mathcal{I} \to L$ *is defined, in order to assure that the postulated model is uniquely solvable.*

Proof. The continuity of the operator ψ is established by first verifying its overall continuity. Given that Ω is constant, the continuity of ψ is consequently ensured.

Let $\tilde{\Phi} = \{\tilde{\Phi} \in \mathcal{I} : \|\tilde{\Phi}\| \leq L, L > 0\}$. Whenever $\tilde{\Phi} \in \mathcal{I}$, we obtain

$$\begin{aligned}
|\psi(\tilde{\Phi})| &= \max_{\tau \in [0,K]} \Bigg| \tilde{\Phi}(0) + \frac{\vartheta \tau^{\vartheta-1}(1-\eta)}{\mathcal{AB}(\eta)} \Omega(\tau, \tilde{\Phi}(\tau)) + \frac{\eta\vartheta}{\lceil \eta \rceil \mathcal{AB}(\eta)} \\
&\quad \times \int_0^\tau m^{\vartheta-1}(\tau - m)^{\eta-1} \Omega(\tau, \tilde{\Phi}(\tau)) dm \Bigg| \\
&\leq \tilde{\Phi}(0) + \frac{\vartheta K^{\vartheta-1}(1-\eta)}{\mathcal{AB}(\eta)} (C_\Phi \|\tilde{\Phi}\| + G_\Phi) + \max_{\tau \in [0,K]} \frac{\eta\vartheta}{\lceil \eta \rceil \mathcal{AB}(\eta)} \\
&\quad \times \int_0^\tau m^{\vartheta-1}(\tau - m)^{\eta-1} |\Omega(m, \tilde{\Phi}(m))| dm \\
|\psi(\tilde{\Phi})| &\leq \tilde{\Phi}(0) + \frac{\vartheta K^{\vartheta-1}(1-\eta)}{\mathcal{AB}(\eta)} (C_\Phi \|\tilde{\Phi}\| + G_\Phi) \\
&\quad + \frac{\eta\vartheta}{\lceil \eta \rceil \mathcal{AB}(\eta)} (C_\Phi \|\tilde{\Phi}\| + G_\Phi) \times K^{\eta+\vartheta-1} \tilde{\Phi}(\eta, \vartheta) \\
&\leq L.
\end{aligned} \tag{7}$$

Thus, if $\tilde{\Phi}(\eta, \vartheta)$ represents a function, the operator ψ is bound by homogeneity. Since ψ is Equi-continuous, when $\tau_1, \tau_2 \leq K$ denote a function. Then consider

$$\begin{aligned}
&|\psi(\tilde{\Phi})(\tau_2) - \psi(\tilde{\Phi})(\tau_1)| \\
&= \Bigg| \frac{\vartheta \tau_2^{\vartheta-1}(1-\eta)}{\mathcal{AB}(\eta)} \Omega(\tau_2, \tilde{\Phi}(\tau_2)) + \frac{\eta\vartheta}{\lceil \eta \rceil \mathcal{AB}(\eta)} \times \int_0^{\tau_2} m^{\vartheta-1}(\tau_2 - m)^{\eta-1} \Omega(m, \tilde{\Phi}(m))\, dm \\
&\quad - \frac{\vartheta \tau_1^{\vartheta-1}(1-\eta)}{\mathcal{AB}(\eta)} \Omega(t_1, \tilde{\Phi}(t_1)) + \frac{\eta\vartheta}{\lceil \eta \rceil \mathcal{AB}(\eta)} \times \int_0^{\tau_1} m^{\vartheta-1}(\tau_1 - m)^{\eta-1} \Omega(m, \tilde{\Phi}(m))\, dm \Bigg| \\
&\leq \frac{\vartheta \tau_2^{\vartheta-1}(1-\eta)}{\mathcal{AB}(\eta)} (C_\Phi \|\tilde{\Phi}\| + G_\Phi) + \frac{\eta\vartheta}{\lceil \eta \rceil \mathcal{AB}(\eta)} (C_\Phi \|\tilde{\Phi}\| + G_\Phi) \times \tau_2^{\eta+\vartheta-1} \tilde{\Phi}(\eta, \vartheta) \\
&\quad - \frac{\vartheta \tau_1^{\vartheta-1}(1-\eta)}{\mathcal{AB}(\eta)} (C_\Phi \|\tilde{\Phi}\| + G_\Phi) + \frac{\eta\vartheta}{\lceil \eta \rceil \mathcal{AB}(\eta)} (C_\Phi \|\tilde{\Phi}\| + G_\Phi) \times \tau_1^{\eta+\vartheta-1} \tilde{\Phi}(\eta, \vartheta).
\end{aligned}$$

When τ_1, τ_2 then $|\psi(\tilde{\Phi})(\tau_2) - \psi(\tilde{\Phi})(\tau_1)| \to 0$.
As a result, we have $\|\psi(\tilde{\Phi})(\tau_2) - \psi(\tilde{\Phi})(\tau_1)\| \to 0$ when $\tau_1 \to \tau_2$.
Due to the fact that ψ is also continuous, Arzela-Ascoli theory is also entirely completely continuous. As such, Schauder's fixed point theorem proves that the suggested model has at least one solution.

Theorem 3. *If condition* (7) *holds such that* $\varpi < 1$, *where*

$$\varpi = \left(\frac{\vartheta K^{\vartheta-1}(1-\eta)}{\mathcal{AB}(\eta)} + \frac{\eta\vartheta}{\lceil\eta\rceil\mathcal{AB}(\eta)} K^{\eta+\vartheta-1} \tilde{\Phi}(\eta,\vartheta) \right) H_\Phi,$$

then the system described by equation (3) *admits a unique solution.*

Proof. Let $\tilde{\Phi}_1, \tilde{\Phi}_2 \in \mathcal{I}$, we have

$$\begin{aligned}
&|\psi(\tilde{\Phi}_1) - \psi(\tilde{\Phi}_2)| \\
&= \max_{\tau\in[0,K]} \left| \frac{\vartheta\tau^{\vartheta-1}(1-\eta)}{\mathcal{AB}(\eta)} \left[\Omega(\tau, \tilde{\Phi}_1(\tau)) - \Omega(\tau, \tilde{\Phi}_2(\tau)) \right] + \frac{\eta\vartheta}{\lceil\eta\rceil\mathcal{AB}(\eta)} \right. \\
&\quad \left. \times \int_0^\tau m^{\vartheta-1}(\tau-m)^{\eta-1}\, dm \left[\Omega(m, \tilde{\Phi}_1(m)) - \Omega(m, \tilde{\Phi}_2(m)) \right] \right| \\
&\leq \left[\frac{\vartheta K^{\vartheta-1}(1-\eta)}{\mathcal{AB}(\eta)} + \frac{\eta\vartheta}{\lceil\eta\rceil\mathcal{AB}(\eta)} K^{\eta+\vartheta-1} \tilde{\Phi}(\eta,\vartheta) \right] \|\tilde{\Phi}_1 - \tilde{\Phi}_2\| \\
&\leq \varpi \|\tilde{\Phi}_1 - \tilde{\Phi}_2\|.
\end{aligned}$$

As a result, the operator ψ qualifies as a contraction, and the model guarantees a unique solution in accordance with the Banach fixed-point theorem.

5.1. Ulam- Hyers Stability

Definition 13. *The model is referred to as Ulam-Hyers stable if, for every small perturbation* $Q(\tau)$ *such that* $|Q(\tau)| \leq \varepsilon$ *for* $\varepsilon > 0$, *there is a unique solution* $P(\tau)$ *such that the approximate solution* $\tilde{\Phi}(\tau)$ *satisfies the inequality*

$$|\tilde{\Phi}(\tau) - P(\tau)| \leq \psi_{\eta,\vartheta}\varepsilon, \quad \textit{for every } \tau \in [0, K].$$

Where $\psi_{\eta,\vartheta}$ *is a constant that dependent on the parameters of the proposed model.*

Now, consider the fractional-order dynamical system governed by

$$({}_0^{FFM}D_\tau^{(\eta,\vartheta)})\tilde{\Phi}(\tau) = \Omega(\tau, \tilde{\Phi}(\tau)) + Q(\tau) \quad \textit{with initial condition} \quad \tilde{\Phi}(0) = \tilde{\Phi}_0.$$

Lemma 1. *Suppose* $P(\tau)$ *is the precise solution to the unperturbed problem, and be the solution of the perturbed problem. Provided* $|Q(\tau)| \leq \varepsilon$, *then*

$$|\tilde{\Phi}(\tau) - P(\tau)| \leq \alpha_{\eta,\vartheta}\varepsilon + \varpi|\tilde{\Phi}(\tau) - P(\tau)|.$$

Proof. This is a very simple illustration. It can be explained by considering (6).

$$({}_0^{FFM})D_\tau^{(\eta,\vartheta)}(\tilde{\Phi}(\tau)-P(\tau))=\Omega(\tau,\tilde{\Phi}(\tau))+Q(\tau)-P(\tau).$$

Applying the Lipschitz condition to Ω:

$$|({}_0^{FFM})D_\tau^{(\eta,\vartheta)}(\tilde{\Phi}(\tau)-P(\tau))|\leq L|\tilde{\Phi}(\tau)-P(\tau)|+|Q(\tau)|.$$

Where L stands for Lipschitz the terms. Expanding the fractional derivative yields

$$\begin{aligned}
&|\tilde{\Phi}(\tau)-P(\tau)|\\
&=\left|\tilde{\Phi}(\tau)-\left(P(0)+\frac{\vartheta\tau^{\vartheta-1}(1-\eta)}{\mathcal{AB}(\eta)}\Omega(\tau,P(\tau))+\frac{\eta\vartheta}{\lceil\eta\rceil\mathcal{AB}(\eta)}\right.\right.\\
&\quad\left.\left.\times\int_0^\tau m^{\vartheta-1}(\tau-m)^{\eta-1}\Omega(m,P(m))\,dm\right)\right|\\
&\leq\frac{\vartheta K^{\vartheta-1}(1-\eta)}{\mathcal{AB}(\eta)}+\frac{\eta\vartheta}{\lceil\eta\rceil\mathcal{AB}(\eta)}K^{\eta+\vartheta-1}\tilde{\Phi}(\eta,\vartheta)+\varpi|\tilde{\Phi}(\tau)-P(\tau)|.
\end{aligned}$$

Satisfies the required criterion

$$|\tilde{\Phi}(\tau)-P(\tau)|\leq\alpha_{\eta,\vartheta}\varepsilon+\varpi|\tilde{\Phi}(\tau)-P(\tau)|,$$

where $\alpha_{\eta,\vartheta}\varepsilon=\frac{\vartheta K^{\vartheta-1}(1-\eta)}{\mathcal{AB}(\eta)}+\frac{\eta\vartheta}{\lceil\eta\rceil\mathcal{AB}(\eta)}K^{\eta+\vartheta-1}\tilde{\Phi}(\eta,\vartheta)$.

Consequently, the proof has been validated.

Lemma 2. *If $\varpi<1$, the suggested model's Ulam-Hyers stable result engages with Lemma 1. The Ulam-Hyers stability for the fractional-order system holds if $\varpi<1$. Under this condition, the perturbed solution $\Upsilon(\tau)$ holds the following:*

$$|\tilde{\Phi}(\tau)-P(\tau)|\leq\frac{\alpha_{\eta,\vartheta}}{1-\varpi}.$$

Proof. From Lemma 1, $|\tilde{\Phi}(\tau)-P(\tau)|\leq\alpha_{\eta,\vartheta}\varepsilon+\varpi|\tilde{\Phi}(\tau)-P(\tau)|$. Another representation of the above relation is in the form

$$|\tilde{\Phi}(\tau)-P(\tau)|\leq\psi_{\eta,\vartheta}\varepsilon,$$

where $\psi_{\eta,\vartheta}=\frac{\alpha_{\eta,\vartheta}}{1-\varpi}$.

The system is shown to be Ulam-Hyers stable using the lemmas hereinabove. The outcome guarantees that any perturbation $Q(\tau)$ produces bounded errors in the solution without affecting system stability.

6. Numerical structure by fractal – fractional representation

The numerical scheme is constructed at the point $\tau = \tau_{d+1}$, permitting an approximate solution of system (3) in terms of Atangana–Baleanu fractal–fractional techniques in the Caputo sense [59].

$$
\begin{aligned}
S_H^{d+1} &= \tilde{S_H}(0,\gamma) + \frac{\vartheta\tau^{\vartheta-1}(1-\eta)}{\mathcal{AB}(\eta)}\kappa_1(\tau_d, S_H^d, I_H^d, T_H^d, R_H^d, P_H^d, S_A^d, I_A^d, R_A^d) \\
&\quad + \frac{\eta\vartheta}{\lceil\eta\rceil\mathcal{AB}(\eta)}\int_0^\tau s^{\vartheta-1}(s-\tau)^{\eta-1} \times \kappa_1(\tau, S_H, I_H, T_H, R_H, P_H, S_A, I_A, R_A)ds \\
I_H^{d+1} &= \tilde{I_H}(0,\gamma) + \frac{\vartheta\tau^{\vartheta-1}(1-\eta)}{\mathcal{AB}(\eta)}\kappa_2(\tau_d, S_H^d, I_H^d, T_H^d, R_H^d, P_H^d, S_A^d, I_A^d, R_A^d) \\
&\quad + \frac{\eta\vartheta}{\lceil\eta\rceil\mathcal{AB}(\eta)}\int_0^\tau s^{\vartheta-1}(s-\tau)^{\eta-1} \times \kappa_2(\tau, S_H, I_H, T_H, R_H, P_H, S_A, I_A, R_A)ds \\
T_H^{d+1} &= \tilde{T_H}(0,\gamma) + \frac{\vartheta\tau^{\vartheta-1}(1-\eta)}{\mathcal{AB}(\eta)}\kappa_3(\tau_d, S_H^d, I_H^d, T_H^d, R_H^d, P_H^d, S_A^d, I_A^d, R_A^d) \\
&\quad + \frac{\eta\vartheta}{\lceil\eta\rceil\mathcal{AB}(\eta)}\int_0^\tau s^{\vartheta-1}(s-\tau)^{\eta-1} \times \kappa_3(\tau, S_H, I_H, T_H, R_H, P_H, S_A, I_A, R_A)ds \\
R_H^{d+1} &= \tilde{R_H}(0,\gamma) + \frac{\vartheta\tau^{\vartheta-1}(1-\eta)}{\mathcal{AB}(\eta)}\kappa_4(\tau_d, S_H^d, I_H^d, T_H^d, R_H^d, P_H^d, S_A^d, I_A^d, R_A^d) \\
&\quad + \frac{\eta\vartheta}{\lceil\eta\rceil\mathcal{AB}(\eta)}\int_0^\tau s^{\vartheta-1}(s-\tau)^{\eta-1} \times \kappa_4(\tau, S_H, I_H, T_H, R_H, P_H, S_A, I_A, R_A)ds \\
P_H^{d+1} &= \tilde{P_H}(0,\gamma) + \frac{\vartheta\tau^{\vartheta-1}(1-\eta)}{\mathcal{AB}(\eta)}\kappa_5(\tau_d, S_H^d, I_H^d, T_H^d, R_H^d, P_H^d, S_A^d, I_A^d, R_A^d) \\
&\quad + \frac{\eta\vartheta}{\lceil\eta\rceil\mathcal{AB}(\eta)}\int_0^\tau s^{\vartheta-1}(s-\tau)^{\eta-1} \times \kappa_5(\tau, S_H, I_H, T_H, R_H, P_H, S_A, I_A, R_A)ds \\
S_A^{d+1} &= \tilde{S_A}(0,\gamma) + \frac{\vartheta\tau^{\vartheta-1}(1-\eta)}{\mathcal{AB}(\eta)}\kappa_6(\tau_d, S_H^d, I_H^d, T_H^d, R_H^d, P_H^d, S_A^d, I_A^d, R_A^d) \\
&\quad + \frac{\eta\vartheta}{\lceil\eta\rceil\mathcal{AB}(\eta)}\int_0^\tau s^{\vartheta-1}(s-\tau)^{\eta-1} \times \kappa_6(\tau, S_H, I_H, T_H, R_H, P_H, S_A, I_A, R_A)ds \\
I_A^{d+1} &= \tilde{I_A}(0,\gamma) + \frac{\vartheta\tau^{\vartheta-1}(1-\eta)}{\mathcal{AB}(\eta)}\kappa_7(\tau_d, S_H^d, I_H^d, T_H^d, R_H^d, P_H^d, S_A^d, I_A^d, R_A^d) \\
&\quad + \frac{\eta\vartheta}{\lceil\eta\rceil\mathcal{AB}(\eta)}\int_0^\tau s^{\vartheta-1}(s-\tau)^{\eta-1} \times \kappa_7(\tau, S_H, I_H, T_H, R_H, P_H, S_A, I_A, R_A)ds \\
R_A^{d+1} &= \tilde{R_A}(0,\gamma) + \frac{\vartheta\tau^{\vartheta-1}(1-\eta)}{\mathcal{AB}(\eta)}\kappa_8(\tau_d, S_H^d, I_H^d, T_H^d, R_H^d, P_H^d, S_A^d, I_A^d, R_A^d) \\
&\quad + \frac{\eta\vartheta}{\lceil\eta\rceil\mathcal{AB}(\eta)}\int_0^\tau s^{\vartheta-1}(s-\tau)^{\eta-1} \times \kappa_8(\tau, S_H, I_H, T_H, R_H, P_H, S_A, I_A, R_A)ds.
\end{aligned}
\tag{8}
$$

From approximating the integrals on the right side of that Equation (8) yields the

following expression.

$$S_H^{d+1} = \tilde{S_H}(0,\gamma) + \frac{\vartheta\tau_d^{\vartheta-1}(1-\eta)}{\mathcal{AB}(\eta)}\kappa_1(\tau_d, S_H^d, I_H^d, T_H^d, R_H^d, P_H^d, S_A^d, I_A^d, R_A^d)$$
$$+ \frac{\eta\vartheta}{\lceil\eta\rceil\mathcal{AB}(\eta)}\sum_{q=0}^{d}\int_{\tau_q}^{\tau_{q+1}} s^{\vartheta-1}(\tau_{d+1}-s)^{\eta-1}\times\kappa_1(\tau, S_H, I_H, T_H, R_H, P_H, S_A, I_A, R_A)\,ds$$

$$I_H^{d+1} = \tilde{I_H}(0,\gamma) + \frac{\vartheta\tau_d^{\vartheta-1}(1-\eta)}{\mathcal{AB}(\eta)}\kappa_2(\tau_d, S_H^d, I_H^d, T_H^d, R_H^d, P_H^d, S_A^d, I_A^d, R_A^d)$$
$$+ \frac{\eta\vartheta}{\lceil\eta\rceil\mathcal{AB}(\eta)}\sum_{q=0}^{d}\int_{\tau_q}^{\tau_{q+1}} s^{\vartheta-1}(\tau_{d+1}-s)^{\eta-1}\times\kappa_2(\tau, S_H, I_H, T_H, R_H, P_H, S_A, I_A, R_A)\,ds$$

$$T_H^{d+1} = \tilde{T_H}(0,\gamma) + \frac{\vartheta\tau_d^{\vartheta-1}(1-\eta)}{\mathcal{AB}(\eta)}\kappa_3(\tau_d, S_H^d, I_H^d, T_H^d, R_H^d, P_H^d, S_A^d, I_A^d, R_A^d)$$
$$+ \frac{\eta\vartheta}{\lceil\eta\rceil\mathcal{AB}(\eta)}\sum_{q=0}^{d}\int_{\tau_q}^{\tau_{q+1}} s^{\vartheta-1}(\tau_{d+1}-s)^{\eta-1}\times\kappa_3(\tau, S_H, I_H, T_H, R_H, P_H, S_A, I_A, R_A)\,ds$$

$$R_H^{d+1} = \tilde{R_H}(0,\gamma) + \frac{\vartheta\tau_d^{\vartheta-1}(1-\eta)}{\mathcal{AB}(\eta)}\kappa_4(\tau_d, S_H^d, I_H^d, T_H^d, R_H^d, P_H^d, S_A^d, I_A^d, R_A^d)$$
$$+ \frac{\eta\vartheta}{\lceil\eta\rceil\mathcal{AB}(\eta)}\sum_{q=0}^{d}\int_{\tau_q}^{\tau_{q+1}} s^{\vartheta-1}(\tau_{d+1}-s)^{\eta-1}\times\kappa_4(\tau, S_H, I_H, T_H, R_H, P_H, S_A, I_A, R_A)\,ds$$

$$P_H^{d+1} = \tilde{P_H}(0,\gamma) + \frac{\vartheta\tau_d^{\vartheta-1}(1-\eta)}{\mathcal{AB}(\eta)}\kappa_5(\tau_d, S_H^d, I_H^d, T_H^d, R_H^d, P_H^d, S_A^d, I_A^d, R_A^d)$$
$$+ \frac{\eta\vartheta}{\lceil\eta\rceil\mathcal{AB}(\eta)}\sum_{q=0}^{d}\int_{\tau_q}^{\tau_{q+1}} s^{\vartheta-1}(\tau_{d+1}-s)^{\eta-1}\times\kappa_5(\tau, S_H, I_H, T_H, R_H, P_H, S_A, I_A, R_A)\,ds$$

$$S_A^{d+1} = \tilde{S_A}(0,\gamma) + \frac{\vartheta\tau_d^{\vartheta-1}(1-\eta)}{\mathcal{AB}(\eta)}\kappa_6(\tau_d, S_H^d, I_H^d, T_H^d, R_H^d, P_H^d, S_A^d, I_A^d, R_A^d)$$
$$+ \frac{\eta\vartheta}{\lceil\eta\rceil\mathcal{AB}(\eta)}\sum_{q=0}^{d}\int_{\tau_q}^{\tau_{q+1}} s^{\vartheta-1}(\tau_{d+1}-s)^{\eta-1}\times\kappa_6(\tau, S_H, I_H, T_H, R_H, P_H, S_A, I_A, R_A)\,ds$$

$$I_A^{d+1} = \tilde{I_A}(0,\gamma) + \frac{\vartheta\tau_d^{\vartheta-1}(1-\eta)}{\mathcal{AB}(\eta)}\kappa_7(\tau_d, S_H^d, I_H^d, T_H^d, R_H^d, P_H^d, S_A^d, I_A^d, R_A^d)$$
$$+ \frac{\eta\vartheta}{\lceil\eta\rceil\mathcal{AB}(\eta)}\sum_{q=0}^{d}\int_{\tau_q}^{\tau_{q+1}} s^{\vartheta-1}(\tau_{d+1}-s)^{\eta-1}\times\kappa_7(\tau, S_H, I_H, T_H, R_H, P_H, S_A, I_A, R_A)\,ds$$

$$R_A^{d+1} = \tilde{R_A}(0,\gamma) + \frac{\vartheta\tau_d^{\vartheta-1}(1-\eta)}{\mathcal{AB}(\eta)}\kappa_8(\tau_d, S_H^d, I_H^d, T_H^d, R_H^d, P_H^d, S_A^d, I_A^d, R_A^d)$$

$$+\frac{\eta\vartheta}{\lceil\eta\rceil\mathcal{AB}(\eta)}\sum_{q=0}^{d}\int_{\tau_q}^{\tau_{q+1}} s^{\vartheta-1}(\tau_{d+1}-s)^{\eta-1}\times\kappa_8(\tau,S_H,I_H,T_H,R_H,P_H,S_A,I_A,R_A)\,ds$$

Afterward, we possess

$$\begin{aligned}
P_q(s) &= \frac{(s-\tau_{q-1})}{(\tau_q-\tau_{q-1})}\tau_q^{\vartheta-1}\kappa_1(\tau_q,S_H^q,I_H^q,T_H^q,R_H^q,P_H^q,S_A^q,I_A^q,R_A^q)\\
&\quad-\frac{(s-\tau_q)}{(\tau_q-\tau_{q-1})}\tau_{q-1}^{\vartheta-1}\kappa_1(\tau_{q-1},S_H^{q-1},I_H^{q-1},T_H^{q-1},R_H^{q-1},P_H^{q-1},S_A^{q-1},I_A^{q-1},R_A^{q-1})\\
Q_q(s) &= \frac{(s-\tau_{q-1})}{(\tau_q-\tau_{q-1})}\tau_q^{\vartheta-1}\kappa_2(\tau_q,S_H^q,I_H^q,T_H^q,R_H^q,P_H^q,S_A^q,I_A^q,R_A^q)\\
&\quad-\frac{(s-\tau_q)}{(\tau_q-\tau_{q-1})}\tau_{q-1}^{\vartheta-1}\kappa_2(\tau_{q-1},S_H^{q-1},I_H^{q-1},T_H^{q-1},R_H^{q-1},P_H^{q-1},S_A^{q-1},I_A^{q-1},R_A^{q-1})\\
U_q(s) &= \frac{(s-\tau_{q-1})}{(\tau_q-\tau_{q-1})}\tau_q^{\vartheta-1}\kappa_3(\tau_q,S_H^q,I_H^q,T_H^q,R_H^q,P_H^q,S_A^q,I_A^q,R_A^q)\\
&\quad-\frac{(s-\tau_q)}{(\tau_q-\tau_{q-1})}\tau_{q-1}^{\vartheta-1}\kappa_3(\tau_{q-1},S_H^{q-1},I_H^{q-1},T_H^{q-1},R_H^{q-1},P_H^{q-1},S_A^{q-1},I_A^{q-1},R_A^{q-1})\\
V_q(s) &= \frac{(s-\tau_{q-1})}{(\tau_q-\tau_{q-1})}\tau_q^{\vartheta-1}\kappa_4(\tau_q,S_H^q,I_H^q,T_H^q,R_H^q,P_H^q,S_A^q,I_A^q,R_A^q)\\
&\quad-\frac{(s-\tau_q)}{(\tau_q-\tau_{q-1})}\tau_{q-1}^{\vartheta-1}\kappa_4(\tau_{q-1},S_H^{q-1},I_H^{q-1},T_H^{q-1},R_H^{q-1},P_H^{q-1},S_A^{q-1},I_A^{q-1},R_A^{q-1})\\
W_q(s) &= \frac{(s-\tau_{q-1})}{(\tau_q-\tau_{q-1})}\tau_q^{\vartheta-1}\kappa_5(\tau_q,S_H^q,I_H^q,T_H^q,R_H^q,P_H^q,S_A^q,I_A^q,R_A^q)\\
&\quad-\frac{(s-\tau_q)}{(\tau_q-\tau_{q-1})}\tau_{q-1}^{\vartheta-1}\kappa_5(\tau_{q-1},S_H^{q-1},I_H^{q-1},T_H^{q-1},R_H^{q-1},P_H^{q-1},S_A^{q-1},I_A^{q-1},R_A^{q-1})\\
X_q(s) &= \frac{(s-\tau_{q-1})}{(\tau_q-\tau_{q-1})}\tau_q^{\vartheta-1}\kappa_6(\tau_q,S_H^q,I_H^q,T_H^q,R_H^q,P_H^q,S_A^q,I_A^q,R_A^q)\\
&\quad-\frac{(s-\tau_q)}{(\tau_q-\tau_{q-1})}\tau_{q-1}^{\vartheta-1}\kappa_6(\tau_{q-1},S_H^{q-1},I_H^{q-1},T_H^{q-1},R_H^{q-1},P_H^{q-1},S_A^{q-1},I_A^{q-1},R_A^{q-1})\\
Y_q(s) &= \frac{(s-\tau_{q-1})}{(\tau_q-\tau_{q-1})}\tau_q^{\vartheta-1}\kappa_7(\tau_q,S_H^q,I_H^q,T_H^q,R_H^q,P_H^q,S_A^q,I_A^q,R_A^q)\\
&\quad-\frac{(s-\tau_q)}{(\tau_q-\tau_{q-1})}\tau_{q-1}^{\vartheta-1}\kappa_7(\tau_{q-1},S_H^{q-1},I_H^{q-1},T_H^{q-1},R_H^{q-1},P_H^{q-1},S_A^{q-1},I_A^{q-1},R_A^{q-1})\\
Z_q(s) &= \frac{(s-\tau_{q-1})}{(\tau_q-\tau_{q-1})}\tau_q^{\vartheta-1}\kappa_8(\tau_q,S_H^q,I_H^q,T_H^q,R_H^q,P_H^q,S_A^q,I_A^q,R_A^q)\\
&\quad-\frac{(s-\tau_q)}{(\tau_q-\tau_{q-1})}\tau_{q-1}^{\vartheta-1}\kappa_8(\tau_{q-1},S_H^{q-1},I_H^{q-1},T_H^{q-1},R_H^{q-1},P_H^{q-1},S_A^{q-1},I_A^{q-1},R_A^{q-1})
\end{aligned}\tag{9}$$

Evaluating the partitioned Lagrange polynomial from Equation (9) provides results,

which are used as the basis for the subsequent numerical analysis.

$$
\begin{aligned}
S_H^{d+1} &= \tilde{S_H}(0,\gamma) + \frac{\vartheta\tau_d^{\vartheta-1}(1-\eta)}{\mathcal{AB}(\eta)} \times \kappa_1(\tau_d, S_H^d, I_H^d, T_H^d, R_H^d, P_H^d, S_A^d, I_A^d, R_A^d) \\
&+ \frac{\vartheta(\delta\tau)^\eta}{\lceil \eta+2 \rceil \mathcal{AB}(\eta)} \times \sum_{q=0}^{d} \Big[\tau_q^{\vartheta-1} \kappa_1(\tau_q, S_H^q, I_H^q, T_H^q, R_H^q, P_H^q, S_A^q, I_A^q, R_A^q) \\
&\times ((d+1-q)^\eta (d-q+2+\eta) - (d-q)(2+2\eta+d-q)) \\
&- \tau_{q-1}^{\vartheta-1} \times \kappa_1(\tau_{q-1}, S_H^{q-1}, I_H^{q-1}, T_H^{q-1}, R_H^{q-1}, P_H^{q-1}, S_A^{q-1}, I_A^{q-1}, R_A^{q-1}) \\
&\times \big((d+1-q)^{\eta+1} - (d-q)^\eta \times (1+\eta+d-q) \big) \Big]. \\
I_H^{d+1} &= \tilde{I_H}(0,\gamma) + \frac{\vartheta\tau_d^{\vartheta-1}(1-\eta)}{\mathcal{AB}(\eta)} \times \kappa_2(\tau_d, S_H^d, I_H^d, T_H^d, R_H^d, P_H^d, S_A^d, I_A^d, R_A^d) \\
&+ \frac{\vartheta(\delta\tau)^\eta}{\lceil \eta+2 \rceil \mathcal{AB}(\eta)} \times \sum_{q=0}^{d} \Big[\tau_q^{\vartheta-1} \kappa_2(\tau_q, S_H^q, I_H^q, T_H^q, R_H^q, P_H^q, S_A^q, I_A^q, R_A^q) \\
&\times ((d+1-q)^\eta (d-q+2+\eta) - (d-q)(2+2\eta+d-q)) \\
&- \tau_{q-1}^{\vartheta-1} \times \kappa_2(\tau_{q-1}, S_H^{q-1}, I_H^{q-1}, T_H^{q-1}, R_H^{q-1}, P_H^{q-1}, S_A^{q-1}, I_A^{q-1}, R_A^{q-1}) \\
&\times \big((d+1-q)^{\eta+1} - (d-q)^\eta \times (1+\eta+d-q) \big) \Big]. \\
T_H^{d+1} &= \tilde{T_H}(0,\gamma) + \frac{\vartheta\tau_d^{\vartheta-1}(1-\eta)}{\mathcal{AB}(\eta)} \times \kappa_3(\tau_d, S_H^d, I_H^d, T_H^d, R_H^d, P_H^d, S_A^d, I_A^d, R_A^d) \\
&+ \frac{\vartheta(\delta\tau)^\eta}{\lceil \eta+2 \rceil \mathcal{AB}(\eta)} \times \sum_{q=0}^{d} \Big[\tau_q^{\vartheta-1} \kappa_3(\tau_q, S_H^q, I_H^q, T_H^q, R_H^q, P_H^q, S_A^q, I_A^q, R_A^q) \\
&\times ((d+1-q)^\eta (d-q+2+\eta) - (d-q)(2+2\eta+d-q)) \\
&- \tau_{q-1}^{\vartheta-1} \times \kappa_3(\tau_{q-1}, S_H^{q-1}, I_H^{q-1}, T_H^{q-1}, R_H^{q-1}, P_H^{q-1}, S_A^{q-1}, I_A^{q-1}, R_A^{q-1}) \\
&\times \big((d+1-q)^{\eta+1} - (d-q)^\eta \times (1+\eta+d-q) \big) \Big]. \\
R_H^{d+1} &= \tilde{R_H}(0,\gamma) + \frac{\vartheta\tau_d^{\vartheta-1}(1-\eta)}{\mathcal{AB}(\eta)} \times \kappa_4(\tau_d, S_H^d, I_H^d, T_H^d, R_H^d, P_H^d, S_A^d, I_A^d, R_A^d) \\
&+ \frac{\vartheta(\delta\tau)^\eta}{\lceil \eta+2 \rceil \mathcal{AB}(\eta)} \times \sum_{q=0}^{d} \Big[\tau_q^{\vartheta-1} \kappa_4(\tau_q, S_H^q, I_H^q, T_H^q, R_H^q, P_H^q, S_A^q, I_A^q, R_A^q) \\
&\times ((d+1-q)^\eta (d-q+2+\eta) - (d-q)(2+2\eta+d-q)) \\
&- \tau_{q-1}^{\vartheta-1} \times \kappa_4(\tau_{q-1}, S_H^{q-1}, I_H^{q-1}, T_H^{q-1}, R_H^{q-1}, P_H^{q-1}, S_A^{q-1}, I_A^{q-1}, R_A^{q-1}) \\
&\times \big((d+1-q)^{\eta+1} - (d-q)^\eta \times (1+\eta+d-q) \big) \Big]. \\
P_H^{d+1} &= \tilde{P_H}(0,\gamma) + \frac{\vartheta\tau_d^{\vartheta-1}(1-\eta)}{\mathcal{AB}(\eta)} \times \kappa_5(\tau_d, S_H^d, I_H^d, T_H^d, R_H^d, P_H^d, S_A^d, I_A^d, R_A^d) \\
&+ \frac{\vartheta(\delta\tau)^\eta}{\lceil \eta+2 \rceil \mathcal{AB}(\eta)} \times \sum_{q=0}^{d} \Big[\tau_q^{\vartheta-1} \kappa_5(\tau_q, S_H^q, I_H^q, T_H^q, R_H^q, P_H^q, S_A^q, I_A^q, R_A^q) \\
&\times ((d+1-q)^\eta (d-q+2+\eta) - (d-q)(2+2\eta+d-q)) \\
&- \tau_{q-1}^{\vartheta-1} \times \kappa_5(\tau_{q-1}, S_H^{q-1}, I_H^{q-1}, T_H^{q-1}, R_H^{q-1}, P_H^{q-1}, S_A^{q-1}, I_A^{q-1}, R_A^{q-1}) \\
&\times \big((d+1-q)^{\eta+1} - (d-q)^\eta \times (1+\eta+d-q) \big) \Big].
\end{aligned}
\tag{10}
$$

$$
\begin{aligned}
S_A^{d+1} &= \tilde{S_A}(0,\gamma) + \frac{\vartheta \tau_d^{\vartheta-1}(1-\eta)}{\mathcal{AB}(\eta)} \times \kappa_6(\tau_d, S_H^d, I_H^d, T_H^d, R_H^d, P_H^d, S_A^d, I_A^d, R_A^d) \\
&\quad + \frac{\vartheta(\delta\tau)^\eta}{\lceil \eta+2 \rceil \mathcal{AB}(\eta)} \times \sum_{q=0}^{d} \Big[\tau_q^{\vartheta-1} \kappa_6(\tau_q, S_H^q, I_H^q, T_H^q, R_H^q, P_H^q, S_A^q, I_A^q, R_A^q) \\
&\quad \times ((d+1-q)^\eta (d-q+2+\eta) - (d-q)(2+2\eta+d-q)) \\
&\quad - \tau_{q-1}^{\vartheta-1} \times \kappa_6(\tau_{q-1}, S_H^{q-1}, I_H^{q-1}, T_H^{q-1}, R_H^{q-1}, P_H^{q-1}, S_A^{q-1}, I_A^{q-1}, R_A^{q-1}) \\
&\quad \times \big((d+1-q)^{\eta+1} - (d-q)^\eta \times (1+\eta+d-q) \big) \Big] . \\
I_A^{d+1} &= \tilde{I_A}(0,\gamma) + \frac{\vartheta \tau_d^{\vartheta-1}(1-\eta)}{\mathcal{AB}(\eta)} \times \kappa_7(\tau_d, S_H^d, I_H^d, T_H^d, R_H^d, P_H^d, S_A^d, I_A^d, R_A^d) \\
&\quad + \frac{\vartheta(\delta\tau)^\eta}{\lceil \eta+2 \rceil \mathcal{AB}(\eta)} \times \sum_{q=0}^{d} \Big[\tau_q^{\vartheta-1} \kappa_7(\tau_q, S_H^q, I_H^q, T_H^q, R_H^q, P_H^q, S_A^q, I_A^q, R_A^q) \\
&\quad \times ((d+1-q)^\eta (d-q+2+\eta) - (d-q)(2+2\eta+d-q)) \\
&\quad - \tau_{q-1}^{\vartheta-1} \times \kappa_7(\tau_{q-1}, S_H^{q-1}, I_H^{q-1}, T_H^{q-1}, R_H^{q-1}, P_H^{q-1}, S_A^{q-1}, I_A^{q-1}, R_A^{q-1}) \\
&\quad \times \big((d+1-q)^{\eta+1} - (d-q)^\eta \times (1+\eta+d-q) \big) \Big] . \\
R_A^{d+1} &= \tilde{R_A}(0,\gamma) + \frac{\vartheta \tau_d^{\vartheta-1}(1-\eta)}{\mathcal{AB}(\eta)} \times \kappa_8(\tau_d, S_H^d, I_H^d, T_H^d, R_H^d, P_H^d, S_A^d, I_A^d, R_A^d) \\
&\quad + \frac{\vartheta(\delta\tau)^\eta}{\lceil \eta+2 \rceil \mathcal{AB}(\eta)} \times \sum_{q=0}^{d} \Big[\tau_q^{\vartheta-1} \kappa_8(\tau_q, S_H^q, I_H^q, T_H^q, R_H^q, P_H^q, S_A^q, I_A^q, R_A^q) \\
&\quad \times ((d+1-q)^\eta (d-q+2+\eta) - (d-q)(2+2\eta+d-q)) \\
&\quad - \tau_{q-1}^{\vartheta-1} \times \kappa_8(\tau_{q-1}, S_H^{q-1}, I_H^{q-1}, T_H^{q-1}, R_H^{q-1}, P_H^{q-1}, S_A^{q-1}, I_A^{q-1}, R_A^{q-1}) \\
&\quad \times \big((d+1-q)^{\eta+1} - (d-q)^\eta \times (1+\eta+d-q) \big) \Big] .
\end{aligned}
$$

7. Results and Discussion

The numerical solutions given in this research provide valuable insights into the transmission dynamics of monkeypox under fuzzy uncertainty and fractional-order modelling. Use of the fractal–fractional method in solving the derived system, that is, Equation (10), offers an efficient paradigm for the solution of the fractional differential equations involved in disease transmission among human and animal populations. Utilizing MATLAB, the simulations incorporate the fuzzified parameters expressed through Triangular Fuzzy Numbers (TFNs) as defined in Definition 2, providing a robust mechanism to capture the uncertainty inherent in real-world epidemiological data. Each parameter's nominal value is obtained through the GMIV (Generalized Mean Integral Value) method outlined in Definition 4, which facilitates the analysis from three key perspectives pessimistic ($m = 0$), moderate ($m = 0.5$), and optimistic ($m = 1$). This methodology makes it possible to gain

deeper insights into how the model outputs are sensitive to different levels of optimism, representing different levels of information available within a vague environment. The parameters utilized in the suggested fuzzy fractional-order monkeypox disease transmission model are presented in Table 1, and the compartmental variations in human and animal populations for different optimism levels $m = 0$, $m = 0.5$, $m = 1$ using triangular fuzzy numbers are shown in Figure 1.

Table 1: Parameter values utilized in the suggested fuzzy fractional-order monkeypox disease transmission model.

Parameter	**Values**
Π_H	0.0056
Π_A	0.002
λ_H	0.004
ξ_H	0.094
Υ_H	0.025
$\mathcal{E}_1$	0.02
$\mathcal{E}_2$	0.01
δ_1	0.005
δ_2	0.001
ω_H	0.04
θ_H	0.02
λ_A	0.015
Υ_A	0.08
μ_H	0.5
μ_A	0.5
d_A	0.2

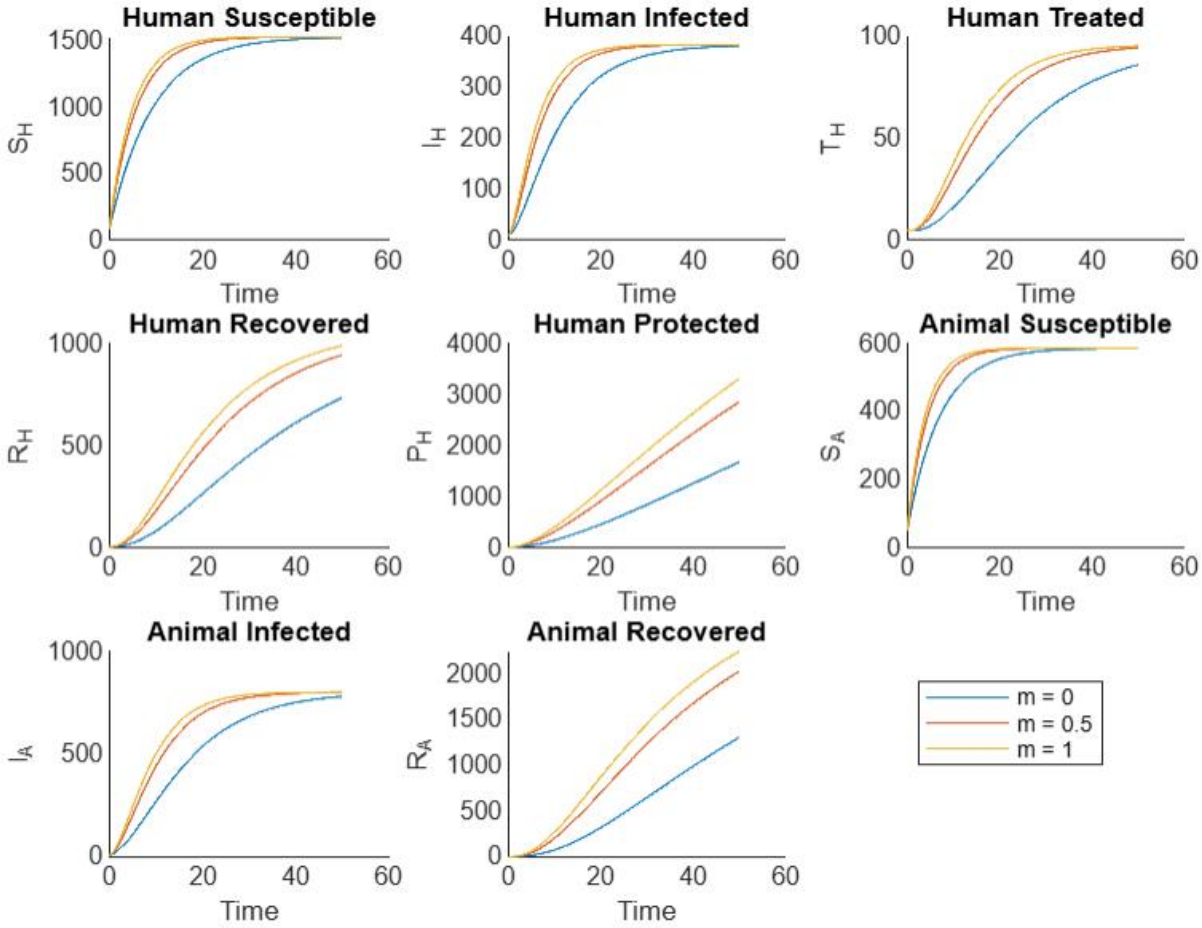

Figure 1: Compartmental variations in human and animal populations for different optimism levels $m = 0$,$m = 0.5$,$m = 1$using triangular fuzzy numbers.

Figure 2 explores the influence of varying fractal dimensions, which represent the environmental complexity and irregular spatial structures impacting disease spread. In the human compartments, the susceptible population shows a varied depletion pattern depending on the fractal geometry, with more irregular environments slowing down exposure. The infected group displays delayed and more dispersed peaks in higher fractal dimensions, highlighting how environmental complexity affects contact and transmission rates. The treatment and recovered compartments are also influenced by fractal structure, with spatial irregularities potentially reducing accessibility to medical care or delaying the healing process. The protected compartment shows mixed behaviour, as its effectiveness depends on how fractal patterns impact the spread and reach of protective measures. Within the animal population, complicated fractal environments are likely to decrease the rate of exposure of susceptible animals to the disease. The infected animal compartment reflects altered peaks based on habitat structure, and the recovery in animals is also sensi-

tive to fractal properties more irregular settings may hinder movement or isolate infected hosts, thus influencing recovery timing.

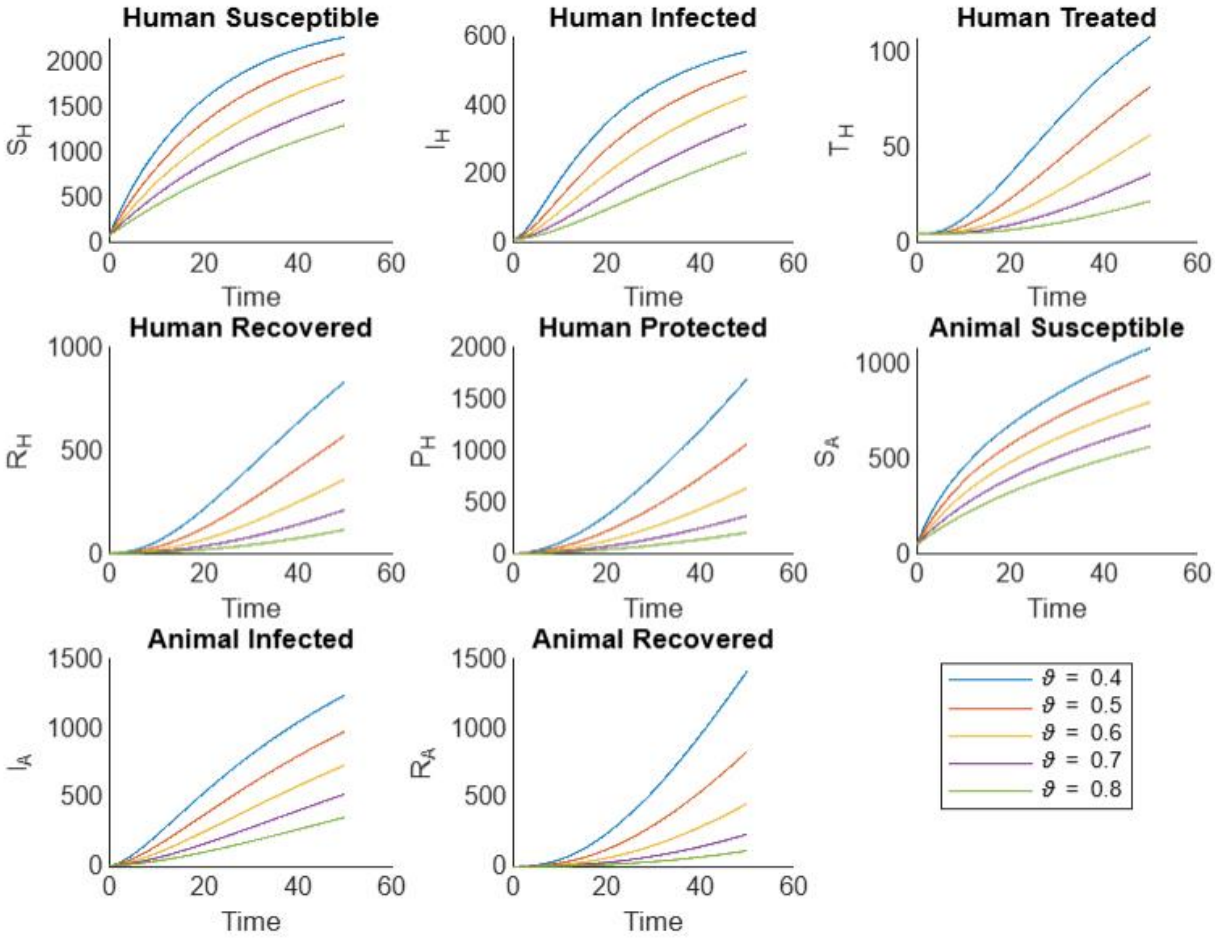

Figure 2: Effect of varying fractal dimensions on the dynamics of human and animal monkeypox compartments.

Figure 3 illustrates the influence of varying fractional orders specifically 0.5, 0.7, and 0.9 on the dynamics of monkeypox transmission in the proposed model. The analysis reveals that incorporating fractional-order derivatives enhances the model's capacity to capture memory and hereditary effects across human and animal compartments. In the human population, increasing the fractional order from 0.5 to 0.9 accelerates the decline of susceptible individuals, indicating that stronger memory effects at higher orders lead to faster responses to infection or preventive measures. Similarly, the infected human compartment decreases more rapidly at higher orders, such as 0.9, reflecting improved adaptability and responsiveness of the system. Treatment and recovery compartments also have more rapid and efficient transitions with increasing order, reflecting diminished

system inertia and better health outcomes. The shielded human group increases more significantly at higher orders, showing more effective immunity accumulation. In the animal compartments, lower fractional order (e.g., 0.5) will result in slower susceptibility reduction and increased infection duration because of enhanced memory retention. A sharper decline in infection and quicker recovery rate is obtained by higher orders (0.7 and 0.9), suggesting improved control and robustness in the animal population.

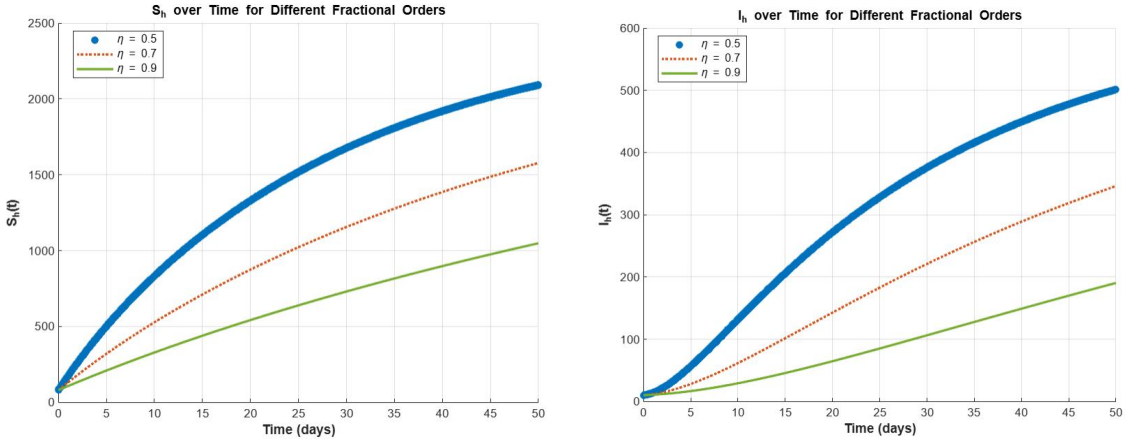

(a) (b)

Figure 3: (a) Effect of various fractional orders on disease development in human and animal populations. (a) Susceptible human in various fractional order, (b) infected human in various fractional order.

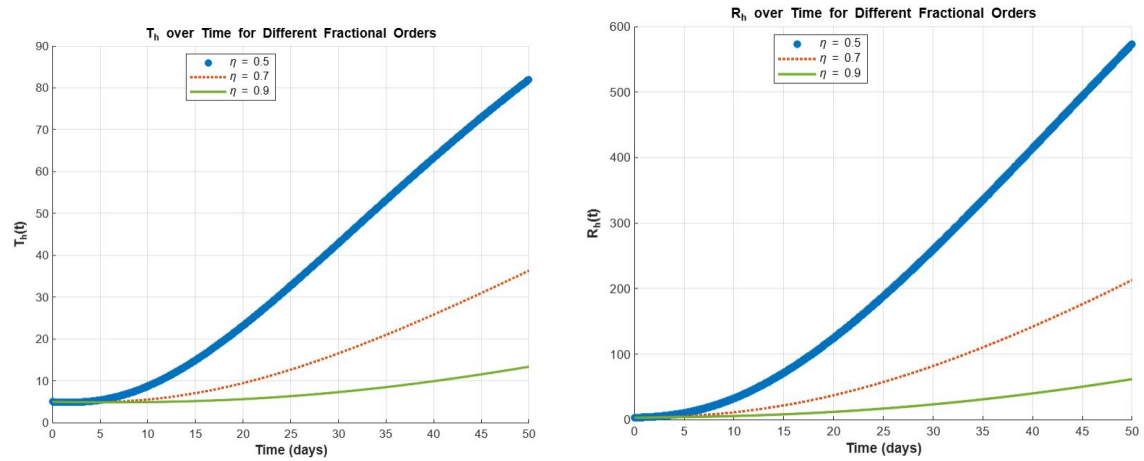

(a) (b)

Figure 4: (a) Treated human in various fractional order, (b) Recovered human in various fractional order.

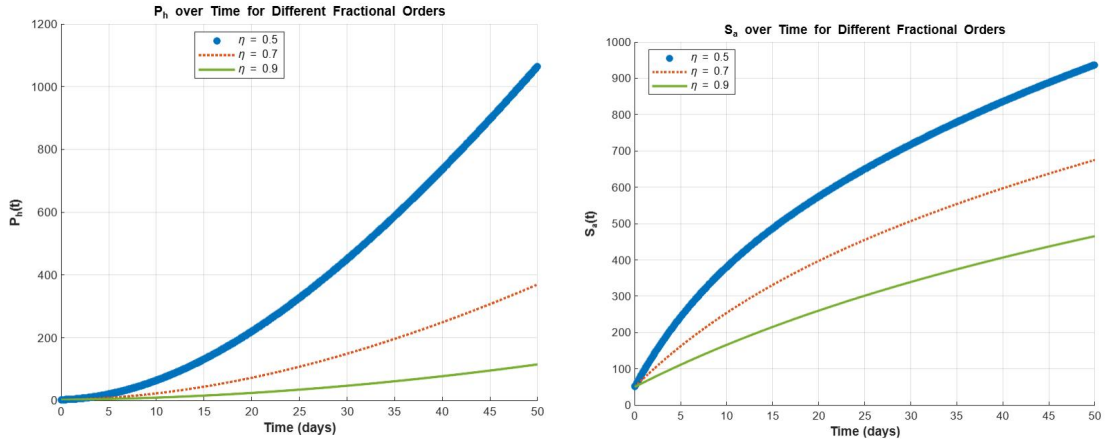

(a) (b)

Figure 5: (a) Protected human in various fractional order. (b) Susceptible animal in various fractional order.

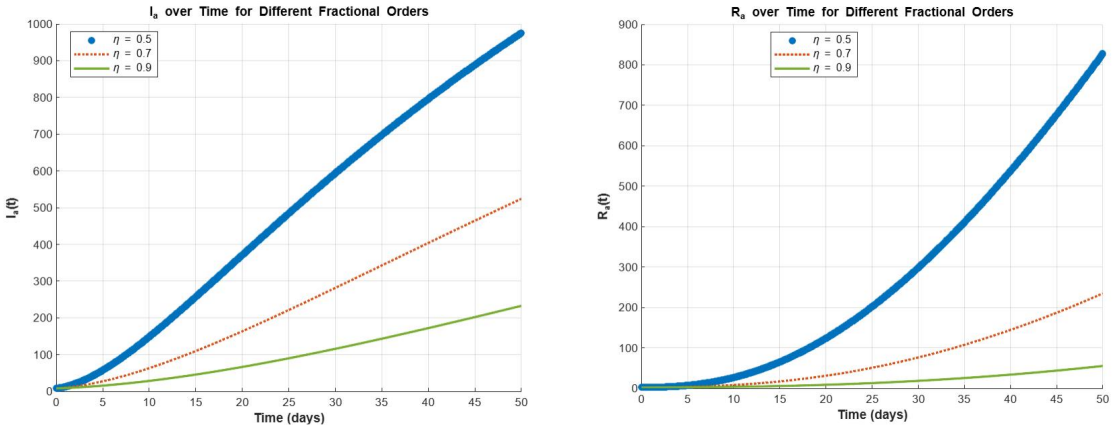

(a) (b)

Figure 6: (a) Infected animal in various fractional order. (b) Recovered animal in various fractional order.

In summary, the combination of fuzzy logic, fractal dimensions, and fractional calculus results in a more complete modelling framework that captures actual-world uncertainty and complexity more reliably than conventional models. This multiple-paradigm strategy increases the sensitivity and responsiveness of epidemiological models, ultimately leading to better-informed and more flexible public health decision-making under uncertainty.

8. Conclusion

In this research, a fuzzy fractal fractional-order model of monkeypox transmission was established that captures parameter uncertainty and memory effects. The findings identify how uncertainty in important parameters like transmission and recovery rates can significantly modify outbreak size and timing and how the incorporation of memory effects indicates that history of past infection continues to influence future epidemic patterns. In capturing imprecise or incomplete data, the model more accurately represents heterogeneity present in real populations. Epidemiologically, this suggests that neglecting uncertainty and memory could underestimate the size and duration of outbreaks. The simulations also give insights into the conditions under which monkeypox propagates rapidly, stabilizes, or disappears, in support of designing effective interventions. Practically, this means that approaches like targeted vaccination, early isolation, and adaptive public health policy should incorporate parameter uncertainty and long-term impacts explicitly in order to enhance outbreak prediction and control. Future research could involve augmenting the framework with optimal control methods and time delays and validating the model using real-world epidemiological data for enhanced predictive ability.

Acknowledgements

Dr .Busayamas Pimpunchat, School of Science, Department of Mathematics,King Mongkut's Institute of Technology Ladkrabang, Bangkok, 10520, Thailand,helped in the completion of this manuscript.

Declaration of competing interest

The authors declare that they have no known competing financial interests or personal relationships that could have appeared to influence the work reported in this paper.

Author's Contribution

All authors contributed equally to the manuscript and typed, read, and approved the final manuscript.

References

[1] P.D.A Qizi. Do you know about monkeypox or mpox? *Multidisciplinary Journal of Science and Technology*, 5(4):908–910, 2025.

[2] Ana Hoxha, Steven M Kerr, Henry Laurenson-Schafer, Nikola Sklenovská, Bernadette Basuta Mirembe, et al. Mpox in children and adolescents during multicountry outbreak, 2022–2023. *Emerging Infectious Diseases*, 29(10):2125, 2023.

[3] Junjie Lu, Hui Xing, Chunhua Wang, Mengjun Tang, Changcheng Wu, Fan Ye, Lijuan Yin, Yang Yang, Wenjie Tan, and Liang Shen. Mpox (formerly monkeypox):

pathogenesis, prevention and treatment. *Signal Transduction and Targeted Therapy*, 8(1):458, 2023.

[4] Aysel Karagoz, Huseyin Tombuloglu, Moneerah Alsaeed, Guzin Tombuloglu, Abdullah A AlRubaish, Amal Mahmoud, Samira Smajlović, Sabahudin Ćordić, Ali A Rabaan, and Ebtesam Alsuhaimi. Monkeypox (mpox) virus: Classification, origin, transmission, genome organization, antiviral drugs, and molecular diagnosis. *Journal of infection and public health*, 16(4):531–541, 2023.

[5] World Health Organization (WHO). Mpox (monkeypox), 2024.

[6] John P Thornhill, Sapha Barkati, Sharon Walmsley, Juergen Rockstroh, Andrea Antinori, Luke B Harrison, Romain Palich, Achyuta Nori, Iain Reeves, Maximillian S Habibi, et al. Monkeypox virus infection in humans across 16 countries—april–june 2022. *New England Journal of Medicine*, 387(8):679–691, 2022.

[7] Mary G Reynolds and Inger K Damon. Outbreaks of human monkeypox after cessation of smallpox vaccination. *Trends in microbiology*, 20(2):80–87, 2012.

[8] Xiefei Yan and Yun Zou. Optimal and sub-optimal quarantine and isolation control in sars epidemics. *Mathematical and computer modelling*, 47(1-2):235–245, 2008.

[9] William Ogilvy Kermack and Anderson G McKendrick. A contribution to the mathematical theory of epidemics. *Proceedings of the royal society of london. Series A, Containing papers of a mathematical and physical character*, 115(772):700–721, 1927.

[10] Anuj Kumar and Prashant K Srivastava. Vaccination and treatment as control interventions in an infectious disease model with their cost optimization. *Communications in Nonlinear Science and Numerical Simulation*, 44:334–343, 2017.

[11] Ririt Andria Sari, Ummu Habibah, and Agus Widodo. Optimal control on model of sars disease spread with vaccination and treatment. *The Journal of Experimental Life Science*, 7(2):61–68, 2017.

[12] Abdelbar El Mansouri, Abderrahim Labzai, Mohamed Belam, and Mostafa Rachik. Mathematical modeling and optimal control strategy for the obesity epidemic. *Commun. Math. Biol. Neurosci.*, 2022:Article–ID, 2022.

[13] Abdelhak Essounaini, Abderrahim Labzai, Hassan Laarabi, and Mostafa Rachik. Mathematical modeling and optimal control strategy for a discrete time model of covid-19 variants. *Commun. Math. Biol. Neurosci.*, 2022:Article–ID, 2022.

[14] Bouchaib Khajji, Driss Kada, Omar Balatif, and Mostafa Rachik. A multi-region discrete time mathematical modeling of the dynamics of covid-19 virus propagation using optimal control. *Journal of Applied Mathematics and Computing*, 64(1):255–281, 2020.

[15] A Labzai, A Kouidere, O Balatif, and M Rachik. Stability analysis of mathematical model new corona virus (covid-19) disease spread in population. *Communications in Mathematical Biology and Neuroscience*, 2020:41, 2020.

[16] B Khajji, L Boujallal, M Elhia, O Balatif, and M Rachik. A fractional-order model for drinking alcohol behaviour leading to road accidents and violence. *Mathematical Modeling and Computing*, 9(3):501–518, 2022.

[17] M Sadki, S Harroudi, and K Allali. Dynamical analysis of an hcv model with cell-to-cell transmission and cure rate in the presence of adaptive immunity. *Mathematical*

Modeling and Computing, 9(3):579–593, 2022.

[18] C Bounkaicha, K Allali, Y Tabit, and J Danane. Global dynamic of spatio-temporal fractional order seir model. *Mathematical Modeling and Computing*, 10(2):299–310, 2023.

[19] M Elkaf and K Allali. Fractional derivative model for tumor cells and immune system competition. *Mathematical Modeling and Computing*, 10(2):288–298, 2023.

[20] Olumuyiwa James Peter, Sumit Kumar, Nitu Kumari, Festus Abiodun Oguntolu, Kayode Oshinubi, and Rabiu Musa. Transmission dynamics of monkeypox virus: a mathematical modelling approach. *Modeling Earth Systems and Environment*, 8(3):3423–3434, 2022.

[21] Pei Yuan, Yi Tan, Liu Yang, Elena Aruffo, Nicholas H Ogden, Jacques Bélair, Jane Heffernan, Julien Arino, James Watmough, Hélène Carabin, et al. Assessing transmission risks and control strategy for monkeypox as an emerging zoonosis in a metropolitan area. *Journal of Medical Virology*, 95(1):e28137, 2023.

[22] Sulaiman Usman, Ibrahim Isa Adamu, et al. Modeling the transmission dynamics of the monkeypox virus infection with treatment and vaccination interventions. *Journal of Applied Mathematics and Physics*, 5(12):2335, 2017.

[23] Olumuyiwa James Peter, Sumit Kumar, Nitu Kumari, Festus Abiodun Oguntolu, Kayode Oshinubi, and Rabiu Musa. Transmission dynamics of monkeypox virus: a mathematical modelling approach. *Modeling Earth Systems and Environment*, 8(3):3423–3434, 2022.

[24] M Ngungu, E Addai, A Adeniji, UM Adam, and K Oshinubi. Mathematical epidemiological modeling and analysis of monkeypox dynamism with non-pharmaceutical intervention using real data from united kingdom. *Frontiers in Public Health*, 11:1101436, 2023.

[25] CP Bhunu and S Mushayabasa. Modelling the transmission dynamics of pox-like infections. 2011.

[26] S Usman and II Adamu. Modeling the transmission dynamics of the monkeypox virus infection with treatment and vaccination interventions. *Journal of Applied Mathematics and Physics*, 5(12):2335, 2017.

[27] Rachel E TeWinkel. *Stability analysis for the equilibria of a monkeypox model*. PhD thesis, The University of Wisconsin-Milwaukee, 2019.

[28] SA Somma, NI Akinwande, and UD Chado. A mathematical model of monkey pox virus transmission dynamics. *Ife Journal of Science*, 21(1):195–204, 2019.

[29] Sai Vikram Bankuru, Samuel Kossol, Wanying Hou, Pooya Mahmoudi, et al. A game-theoretic model of monkeypox to assess vaccination strategies. *PeerJ*, 8:e9272, 2020.

[30] Rebecca Grant, Le Bao Long Nguyen, and Romulus Breban. Modelling human-to-human transmission of monkeypox. *Bulletin of the World Health Organization*, 98(9):638, 2020.

[31] Fathalla A Rihan, Dumitru Baleanu, S Lakshmanan, and R Rakkiyappan. On fractional sirc model with salmonella bacterial infection. *Abstract and Applied Analysis*, 2014, 2014.

[32] Ismaila A Baba and Bappah Garba Nasidi. Fractional order epidemic model for the dynamics of novel covid-19. *Alexandria Engineering Journal*, 60(1):537–548, 2021.

[33] Fathalla A Rihan. Numerical modeling of fractional-order biological systems. *Abstract and Applied Analysis*, 2013, 2013.

[34] Asif Ali, Saeed Ullah, and Muhammad Altaf Khan. The impact of vaccination on the modeling of covid-19 dynamics: a fractional order model. *Nonlinear Dynamics*, 110(4):3921–3940, 2022.

[35] M Saeedian, M Khalighi, N Azimi-Tafreshi, GR Jafari, and M Ausloos. Memory effects on epidemic evolution: The susceptible-infected-recovered epidemic model. *Physical Review E*, 95(2):022409, 2017.

[36] I Ahmed, IA Baba, A Yusuf, P Kumam, and W Kumam. Analysis of caputo fractional-order model for covid-19 with lockdown. *Advances in Difference Equations*, 2020(1):1–19, 2020.

[37] Muhammad A Aba Oud, Asif Ali, Hashim Alrabaiah, Saeed Ullah, et al. A fractional order mathematical model for covid-19 dynamics with quarantine, isolation, and environmental viral load. *Advances in Difference Equations*, 2021(1):1–19, 2021.

[38] Muhammad Altaf Khan, Saeed Ullah, and Sunil Kumar. A robust study on 2019-ncov outbreaks through non-singular derivative. *The European Physical Journal Plus*, 136(2):168, 2021.

[39] Adnan Khan, Yassine Sabbar, and Anwarud Din. Stochastic modeling of the monkeypox 2022 epidemic with cross-infection hypothesis in a highly disturbed environment. *Mathematical Biosciences and Engineering*, 19(12):13560–13581, 2022.

[40] Alaa M Alzubaidi, Hind A Othman, Saeed Ullah, Nafees Ahmad, and Muhammad Zubair Alam. Analysis of monkeypox viral infection with human to animal transmission via a fractional and fractal-fractional operators with power law kernel. *Mathematical Biosciences and Engineering*, 20(4):6666–6690, 2023.

[41] Joshua Kiddy K Asamoah, Eric Okyere, Ernest Yankson, Alex A Opoku, et al. Non-fractional and fractional mathematical analysis and simulations for q fever. *Chaos, Solitons & Fractals*, 156:111821, 2022.

[42] Sunil Kumar, Subir Ghosh, Ranjan Kumar, and Mohamed Jleli. A fractional model for population dynamics of two interacting species by using spectral and hermite wavelets methods. *Numerical Methods for Partial Differential Equations*, 37(2):1652–1672, 2021.

[43] Abdon Atangana and J F Gómez-Aguilar. A new derivative with normal distribution kernel: Theory, methods and applications. *Physica A: Statistical Mechanics and its Applications*, 476:1–14, 2017.

[44] Oluwole Daniel Peter, Faith A Oguntolu, Mufutau M Ojo, A Olayinka Oyeniyi, Rashid Jan, and Ilyas Khan. Fractional order mathematical model of monkeypox transmission dynamics. *Physica Scripta*, 97(8):084005, 2022.

[45] OJ Peter, S Kumar, N Kumari, FA Oguntolu, K Oshinubi, and R Musa. Transmission dynamics of monkeypox virus: a mathematical modeling approach. *Modeling Earth Systems and Environment*, 8(3):3423–3434, 2022.

[46] Subrata Adak and Soovoojeet Jana. Dynamical behavior of an epidemic model with

fuzzy transmission and fuzzy treatment control. *Journal of Applied Mathematics and Computing*, 68(3):1929–1948, 2022.

[47] Saba Riaz, Asif Ali, and Maria Munir. Sensitivity analysis of an infectious disease model under fuzzy impreciseness. *Partial Differential Equations in Applied Mathematics*, 9:100638, 2024.

[48] V Padmapriya and M Kaliyappan. Fuzzy fractional mathematical model of covid-19 epidemic. *Journal of Intelligent & Fuzzy Systems*, 42(4):3299–3321, 2022.

[49] A Hanif, Arshad Riaz Khan Butt, S Ahmad, Rafi Ud Din, and Mustafa Inc. A new fuzzy fractional order model of transmission of covid-19 with quarantine class. *The European Physical Journal Plus*, 136(11):1–28, 2021.

[50] S Chakraverty, RM Jena, and SK Jena. Fuzzy time-fractional sirs-si malaria disease model. In *Time-Fractional Order Biological Systems with Uncertain Parameters*, pages 123–142. Springer, 2020.

[51] Tofigh Allahviranloo. *Fuzzy fractional differential operators and equations*. Springer, 2021.

[52] Leila Safikhani, Tofigh Allahviranloo, Ljerka Mrsic, and Shyamal Samanta. Numerical solution for fuzzy fractional differential equations by fuzzy multi-step methods. *Symmetry*, 17(4):545, 2025.

[53] Irina Perfilieva. Fuzzy transforms: Theory and applications. *Fuzzy Sets and Systems*, 157(3):993–1023, 2006.

[54] Osmo Kaleva. Fuzzy differential equations. *Fuzzy Sets and Systems*, 24(3):301–317, 1987.

[55] S Arshad and V Lupulescu. Fractional differential equation with the fuzzy initial condition. *Electronic Journal of Differential Equations*, 2011(34):1–15, 2011.

[56] Kwang H Lee. Fuzzy function. In *First Course on Fuzzy Theory and Applications*, pages 153–170. Springer, 2005.

[57] Laécio Carvalho de Barros, Rodney Carlos Bassanezi, and Weldon Alexander Lodwick. *A first course in fuzzy logic, fuzzy dynamical systems, and biomathematics: Theory and applications*. Springer, 2017.

[58] Prasenjit Mahato, Subhashis Das, and Sanat Kumar Mahato. An epidemic model through information-induced vaccination and treatment under fuzzy impreciseness. *Modeling Earth Systems and Environment*, 8(3):2863–2887, 2022.

[59] Abdon Atangana. Fractal-fractional differentiation and integration: connecting fractal calculus and fractional calculus to predict complex system. *Chaos, Solitons & Fractals*, 102:396–406, 2017.

[60] Shao-Wen Yao, A Ahmad, M Inc, M Farman, A Ghaffar, and A Akgul. Analysis of fractional order diarrhea model using fractal fractional operator. *Fractals*, 30(05):2240173, 2022.